Electronic Supplementary Material (ESI) for Dalton Transactions.

Asymmetric Charge Separation and Recombination in Symmetrically Functionalized σ-π Hybrid Oligosilanes

Jiawang Zhou, Carlton P. Folster, Sravan K. Surampudi, Daniel Jimenez, Rebekka S. Klausen*, Arthur E. Bragg*

Department of Chemistry, Johns Hopkins University, 3400 N. Charles St. Baltimore, MD 21218

klausen@jhu.edu, artbragg@jhu.edu

Table of Contents

1. General Information

General Experimental Procedures: All experiments were performed under an atmosphere of dry nitrogen or argon with the rigid exclusion of air and moisture using standard Schlenk techniques or in a nitrogen glove box. All glassware was oven-dried overnight in a 175 °C oven.

Instrumentation: ^{1}H NMR, ^{13}C {^{1}H} NMR, and ^{29}Si {^{1}H} DEPT NMR were recorded on either a Bruker Avance 300 or 400 MHz spectrometer and chemical shifts are reported in parts per million (ppm). Spectra were recorded in benzene-*d_6* or chloroform-*d* with tetramethylsilane or the residual solvent peak as the internal standard (^{1}H NMR: C_6H_6 δ = 7.16; $CHCl_3$, δ = 7.26). Multiplicities are as indicated: s (singlet), d (doublet), t (triplet), dd (doublet of doublets), m (multiplet), and br (broad). Coupling constants, J, are reported in Hertz and integration is provided. Mass Spectrometry (MS) and High Resolution Mass Spectrometry (HRMS) were either performed in the Department of Chemistry at Johns Hopkins University using a VG Instruments VG70S/E magnetic sector mass spectrometer with EI (70 eV) or in the Columbia University Department of Chemistry mass spectrometry facility using a Waters XEVO G2XS QToF mass spectrometer equipped with a UPC2 SFC inlet, electrospray ionization (ESI) probe, atmospheric pressure chemical ionization (APCI) probe, and atmospheric solids analysis probe (ASAP). Elemental analysis was performed by Robertson Microlit Laboratories.

2. NMR Spectra

2.1 NMR Spectra of Compound **3**

2.1.1 ^{1}H NMR Spectrum (400 MHz, $CDCl_3$)

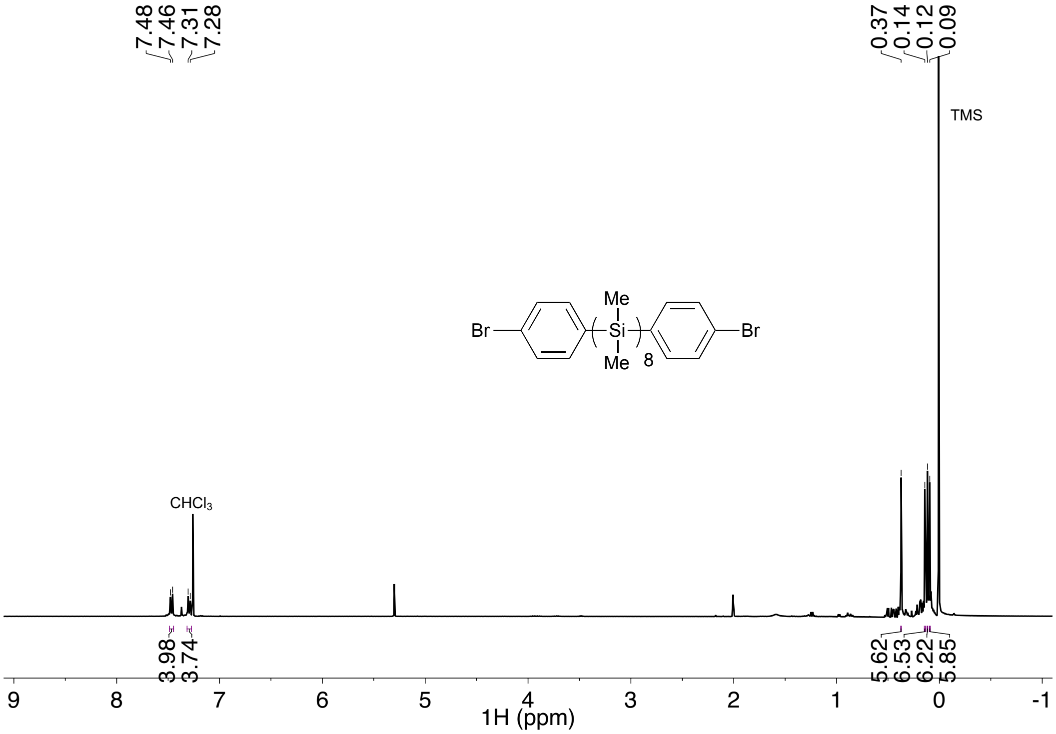

2.1.2 ^{13}C NMR Spectrum (101 MHz, $CDCl_3$)

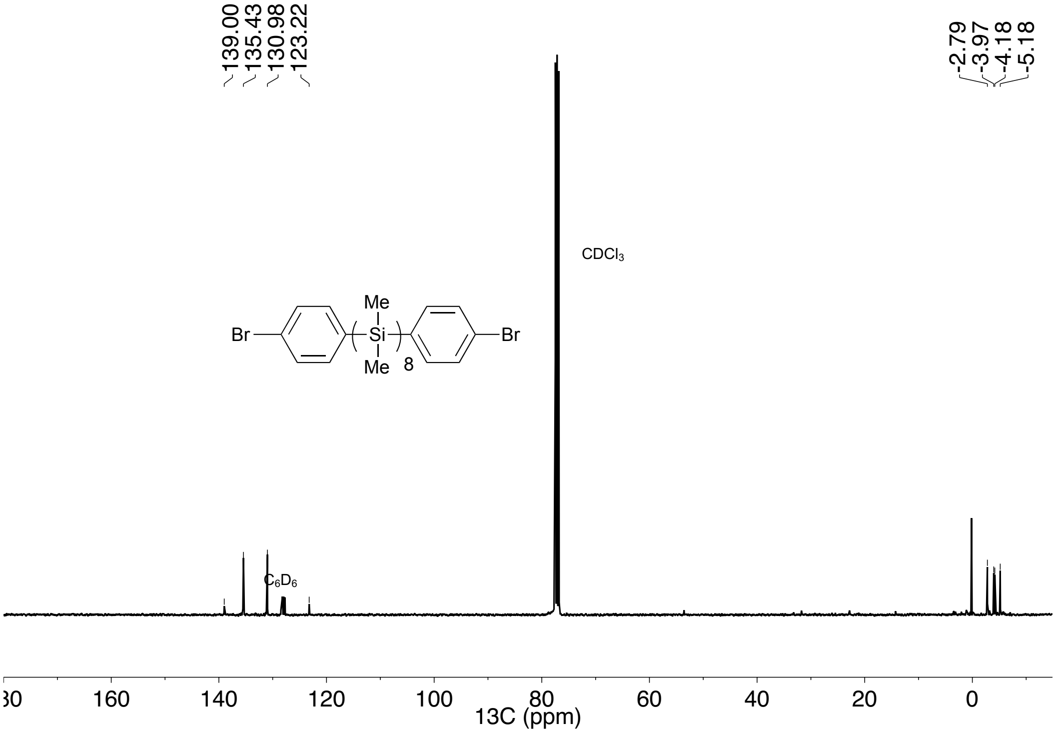

2.1.3 ^{29}Si NMR Spectrum (79 MHz, $CDCl_3$)

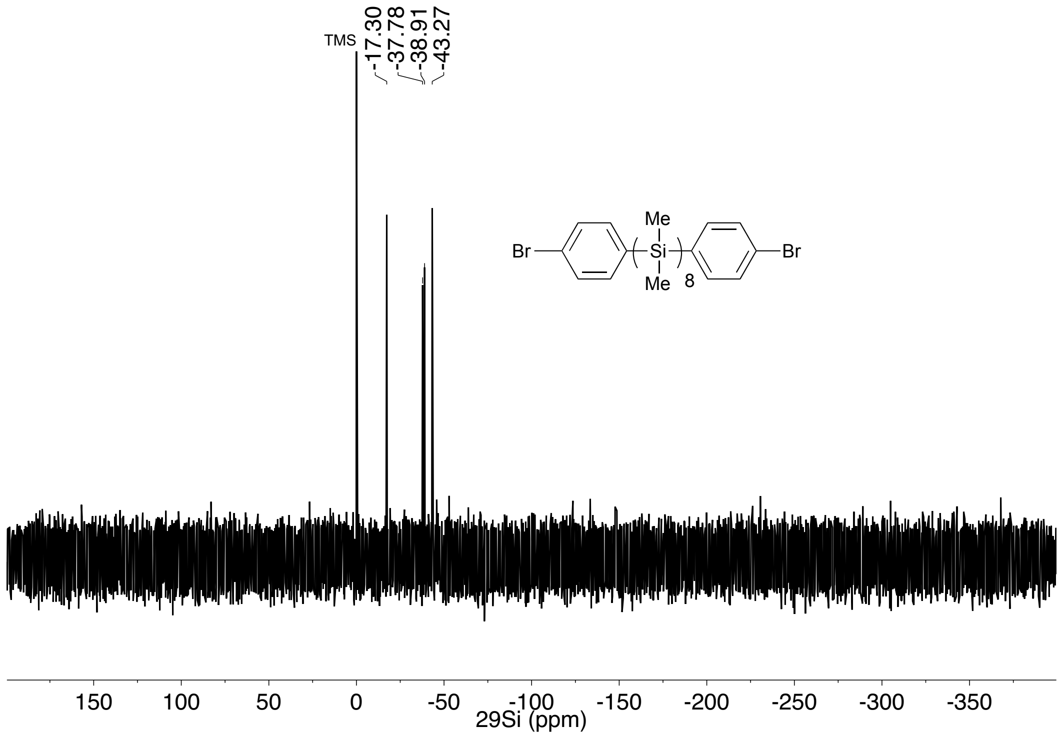

2.2 NMR Spectra of Compound **5**

2.2.1 ^{1}H NMR Spectrum (400 MHz, $CDCl_3$)

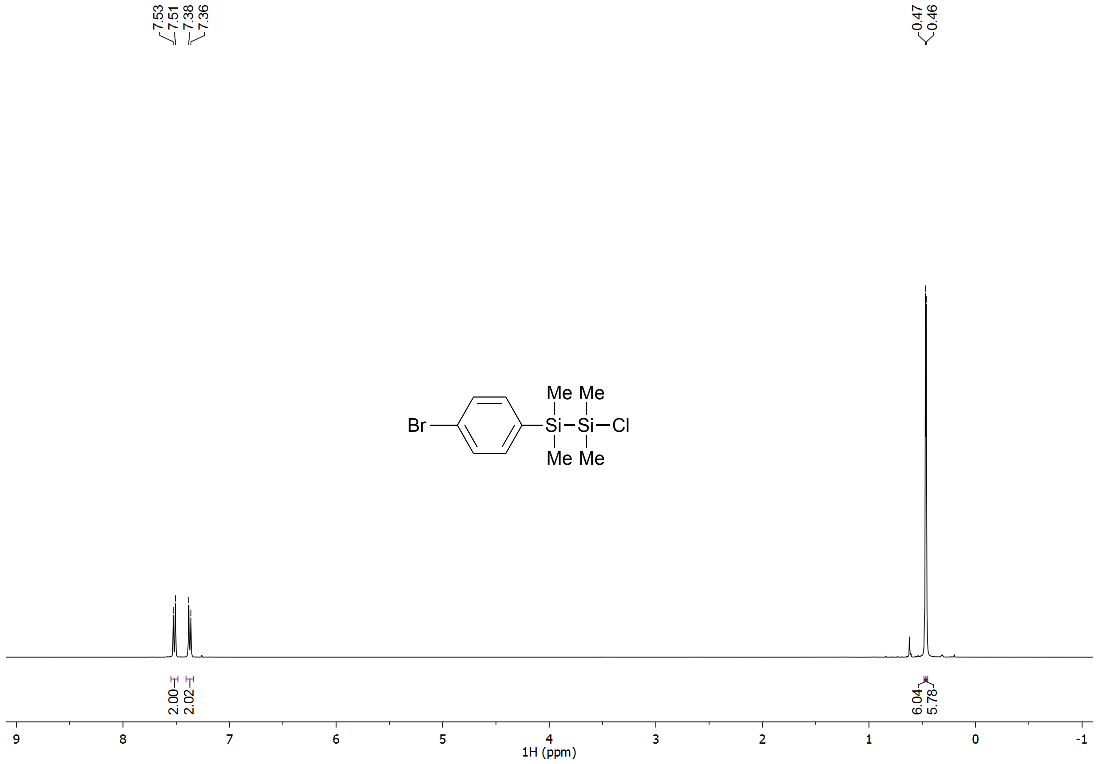

2.2.2 ^{29}Si NMR Spectrum (79 MHz, $CDCl_3$)

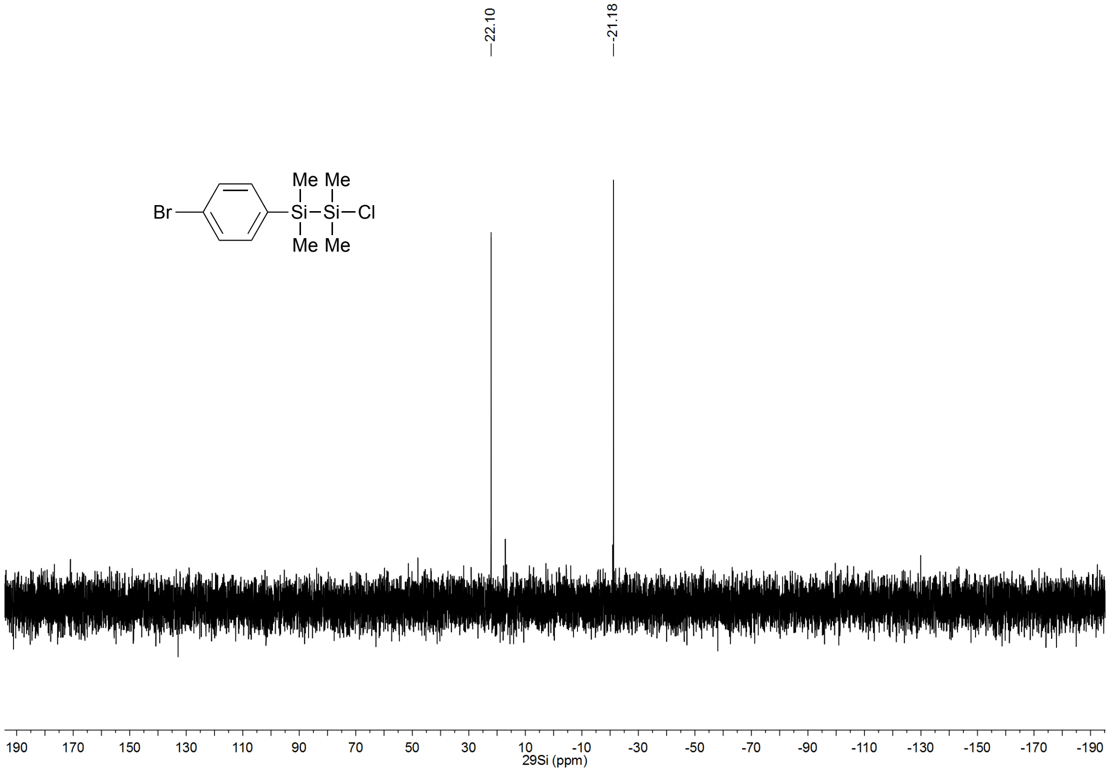

2.3 NMR Spectra of Compound **6**

2.3.1 ^{1}H NMR Spectrum (400 MHz, C_6D_6)

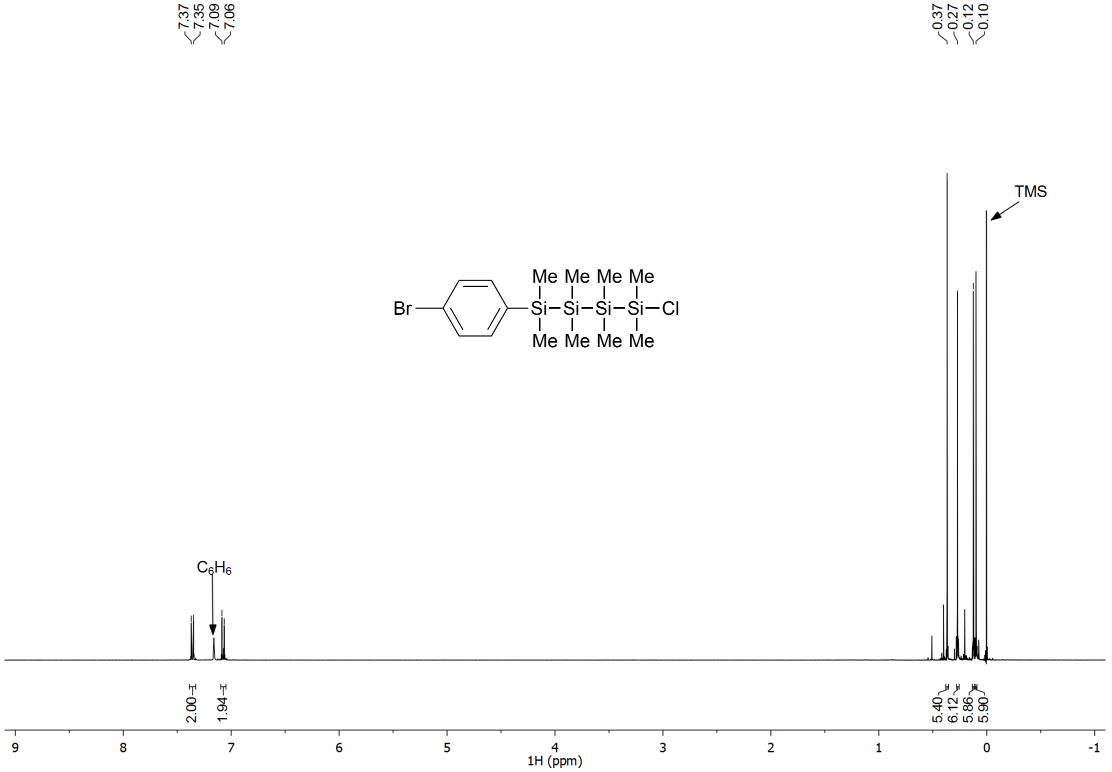

2.3.2 ^{13}C NMR Spectrum (101 MHz, C_6D_6)

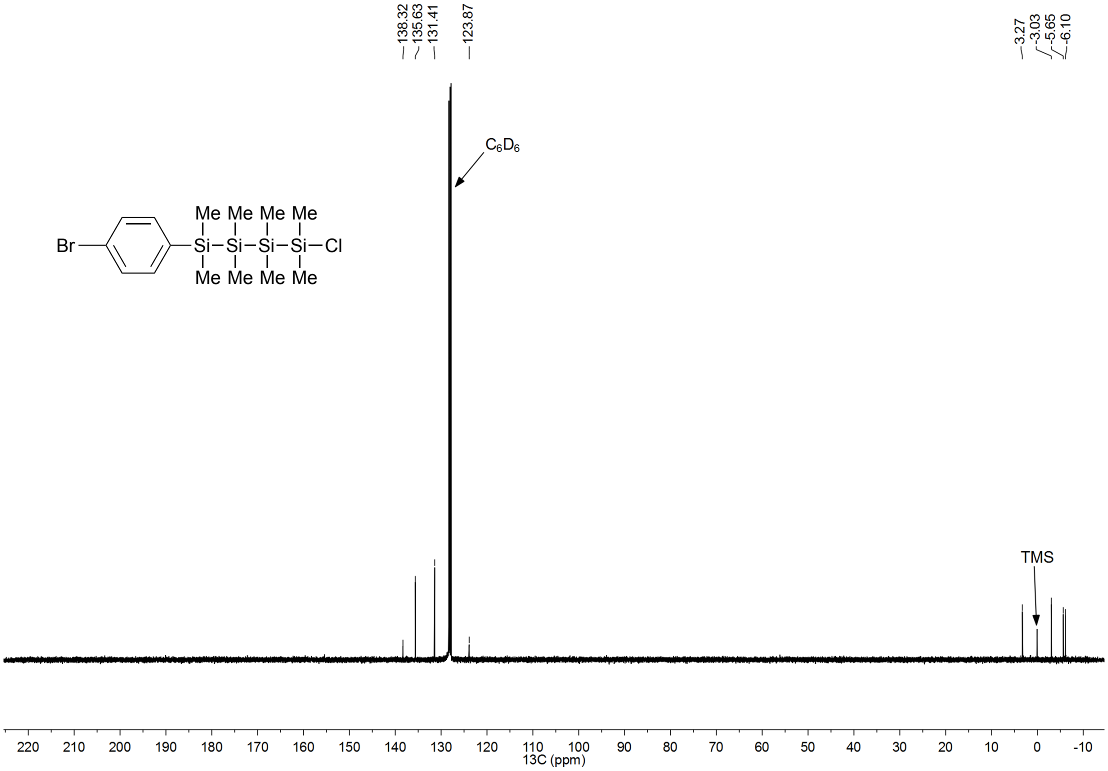

2.3.3 ^{29}Si NMR Spectrum (79 MHz, C_6D_6)

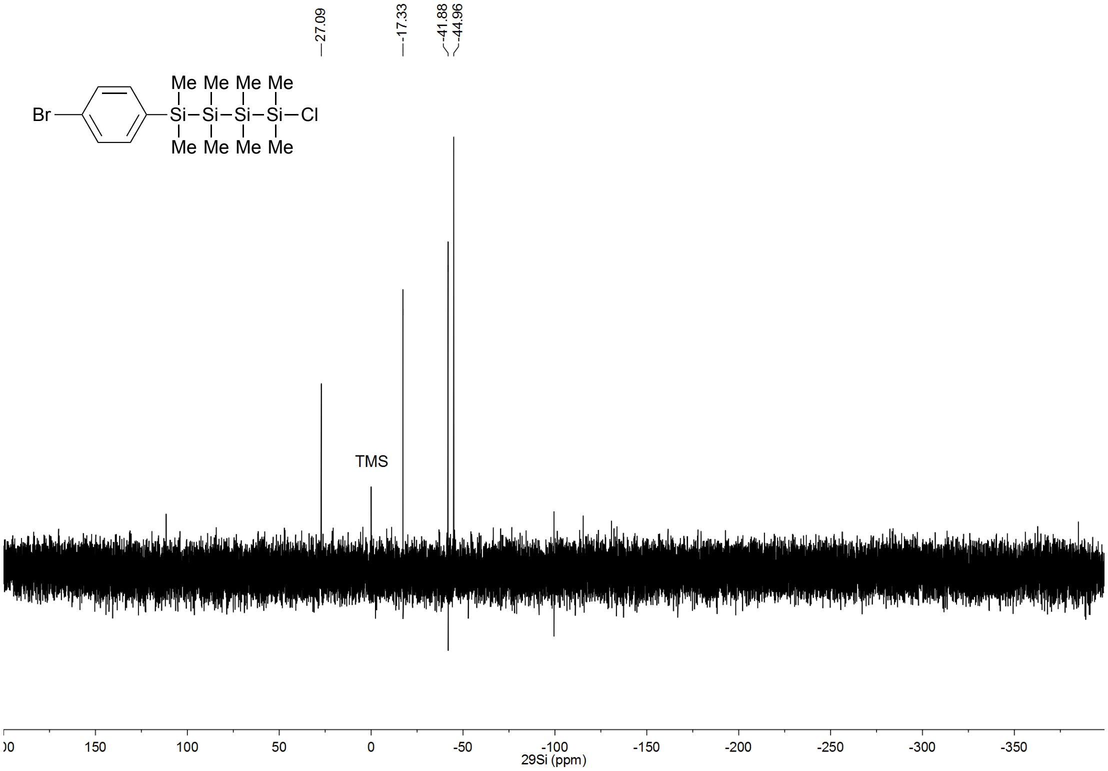

2.4 NMR Spectra of Compound **7**

2.4.1 ^{1}H NMR Spectrum (400 MHz, CDCl$_3$)

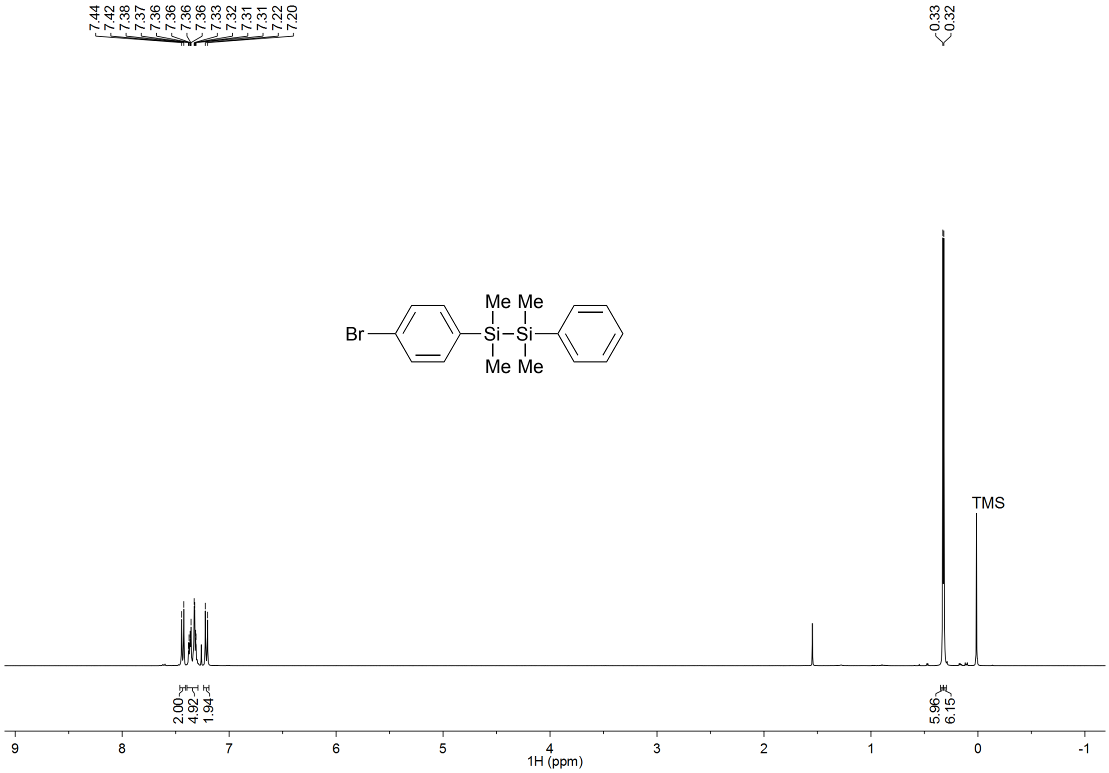

2.4.2 ^{13}C NMR Spectrum (101 MHz, CDCl$_3$)

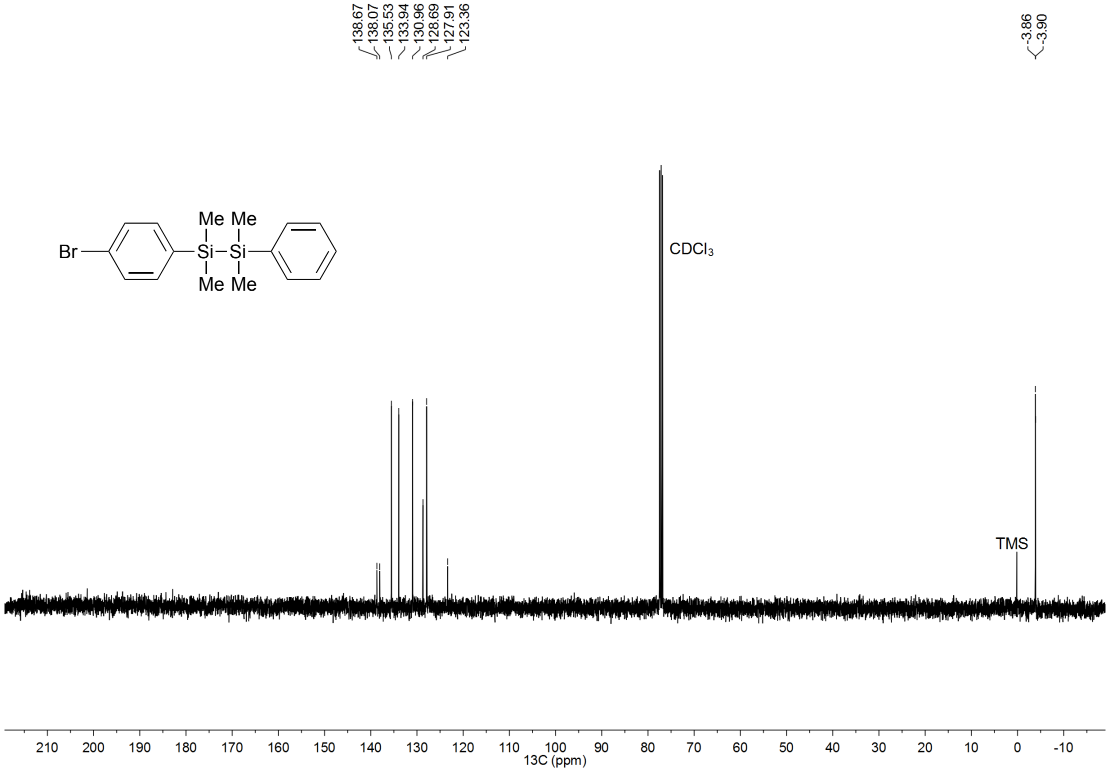

2.4.3 ^{29}Si NMR Spectrum (79 MHz, $CDCl_3$)

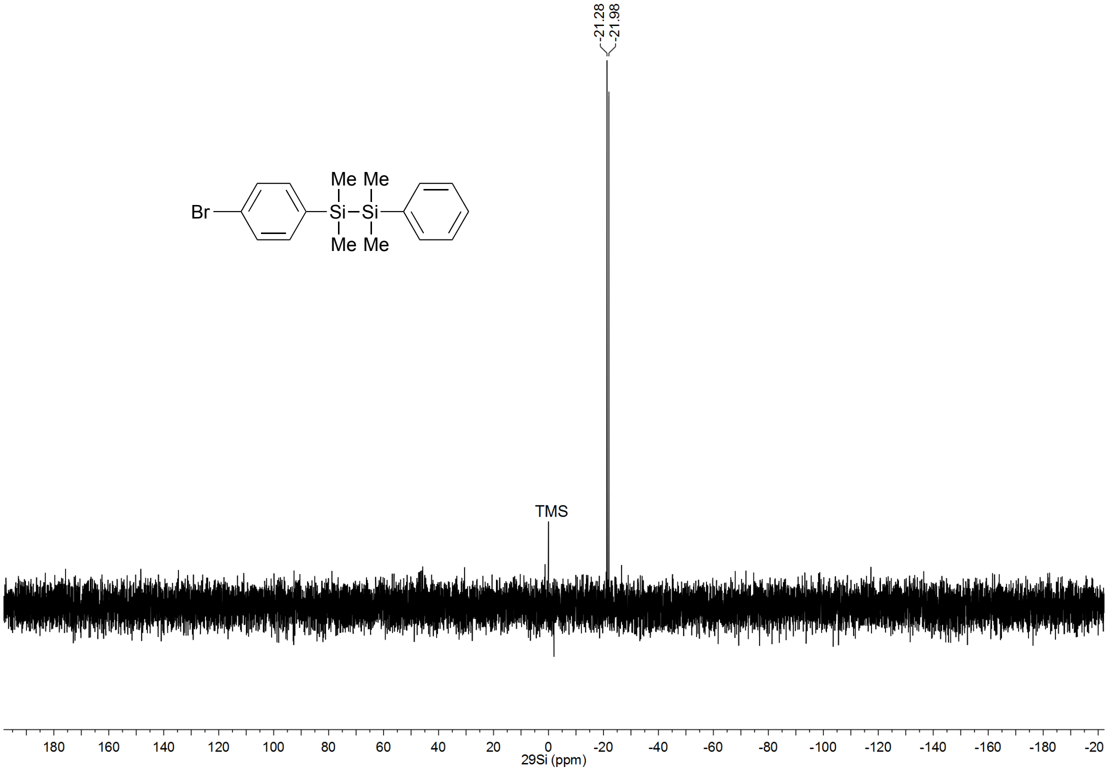

2.5 NMR Spectra of Compound **8**

2.5.1 ^{1}H NMR Spectrum (400 MHz, C_6D_6)

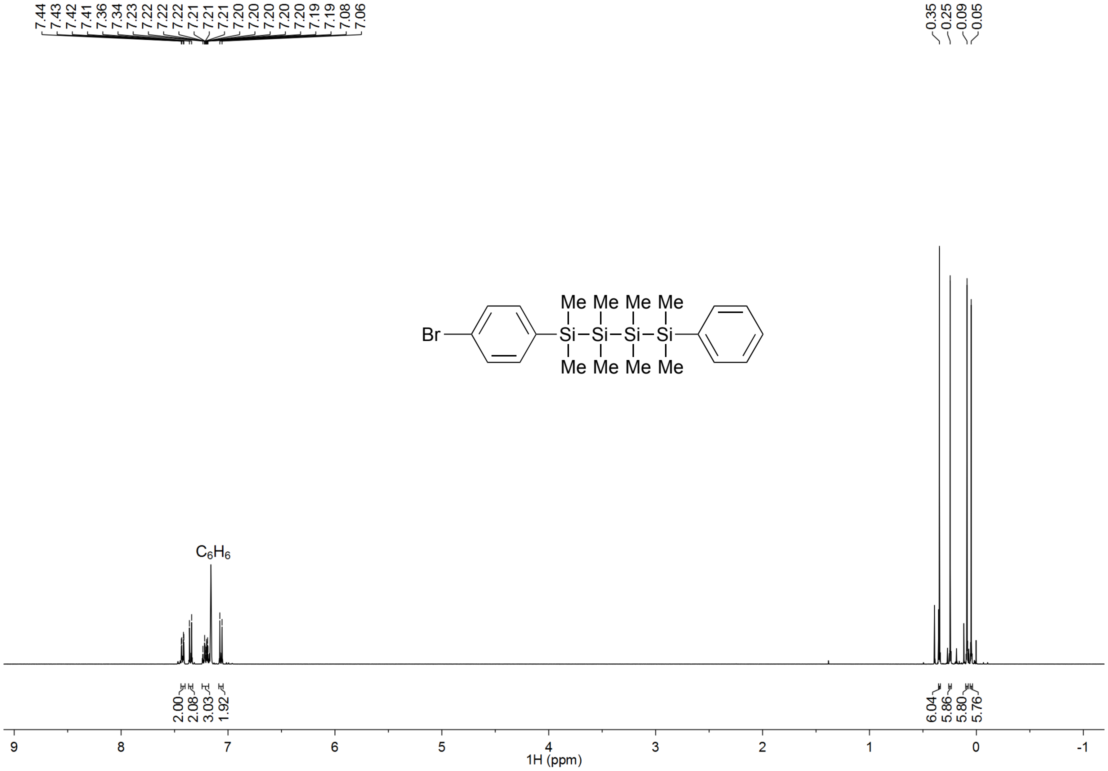

2.5.2 ^{13}C NMR Spectrum (75 MHz, C_6D_6)

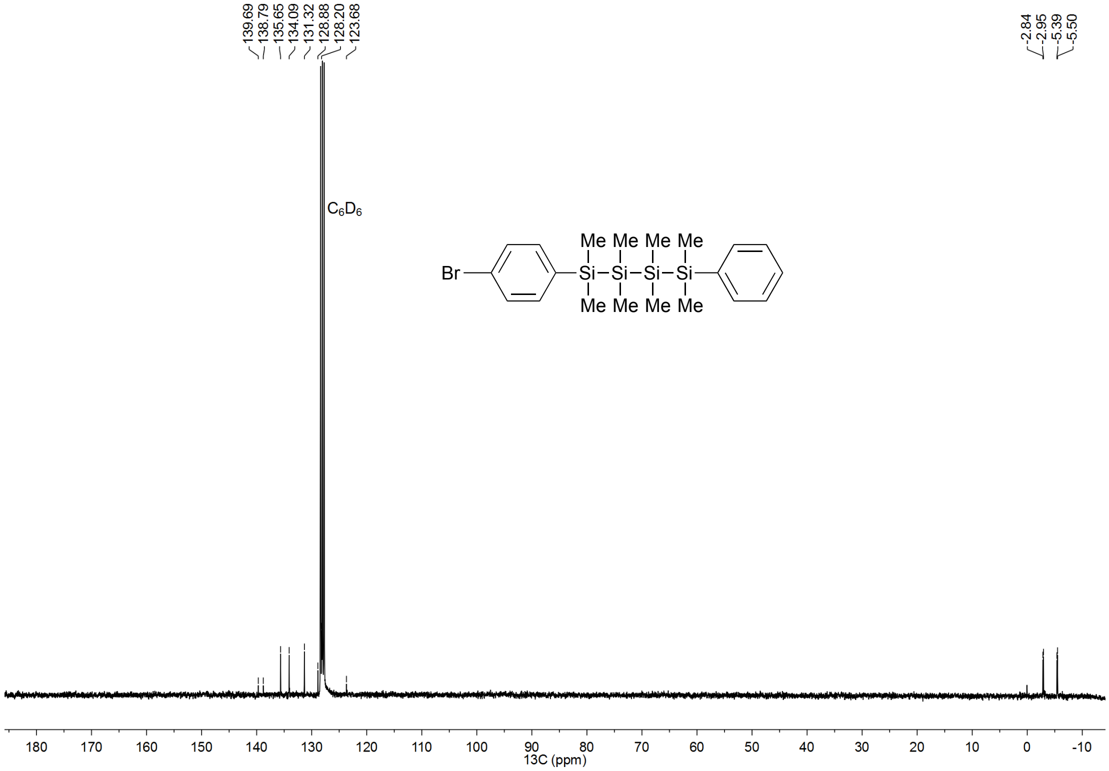

2.5.3 ^{29}Si NMR Spectrum (79 MHz, C_6D_6)

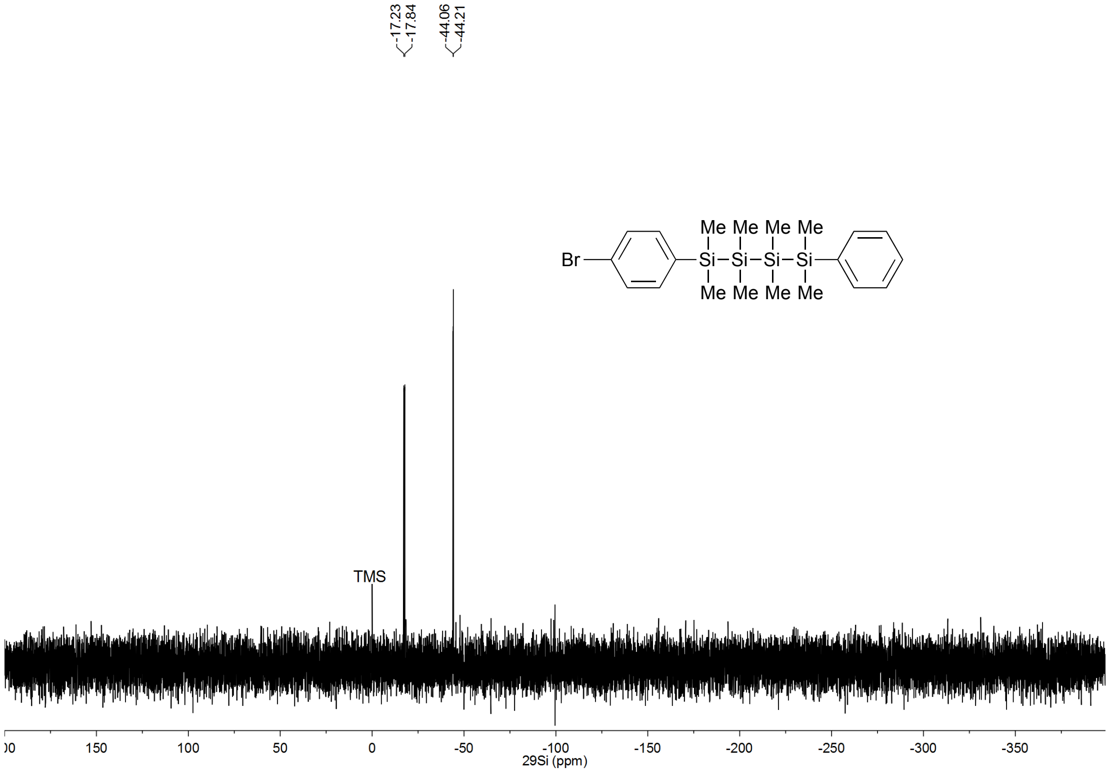

2.6 NMR Spectra of Compound **4**

2.6.1 ^{1}H NMR Spectrum (400 MHz, $CDCl_3$)

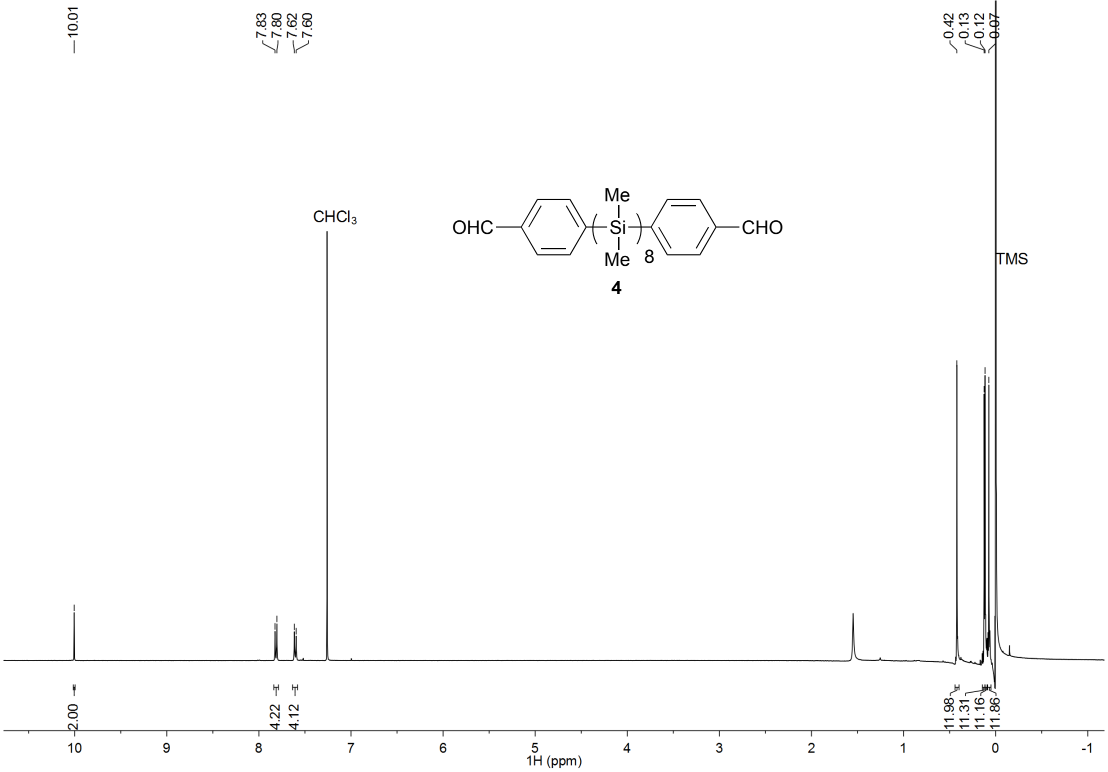

2.6.2 ^{13}C NMR Spectrum (101 MHz, $CDCl_3$)

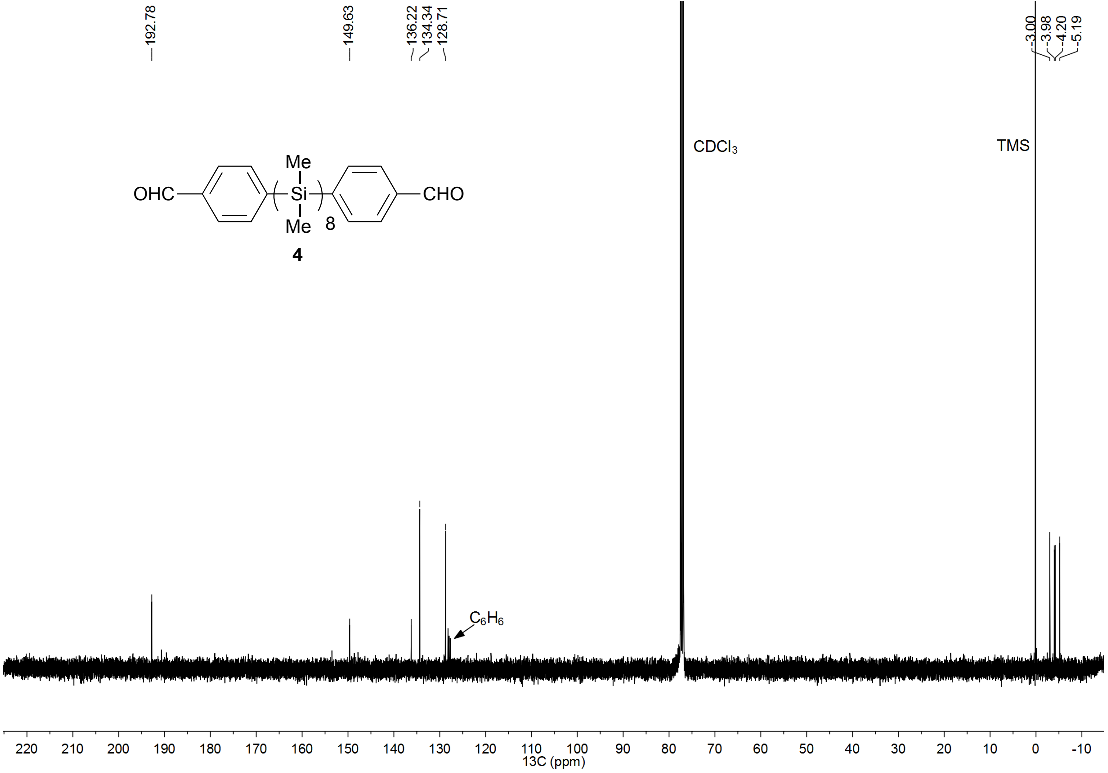

2.6.3 ^{29}Si NMR Spectrum (79 MHz, CDCl$_3$)

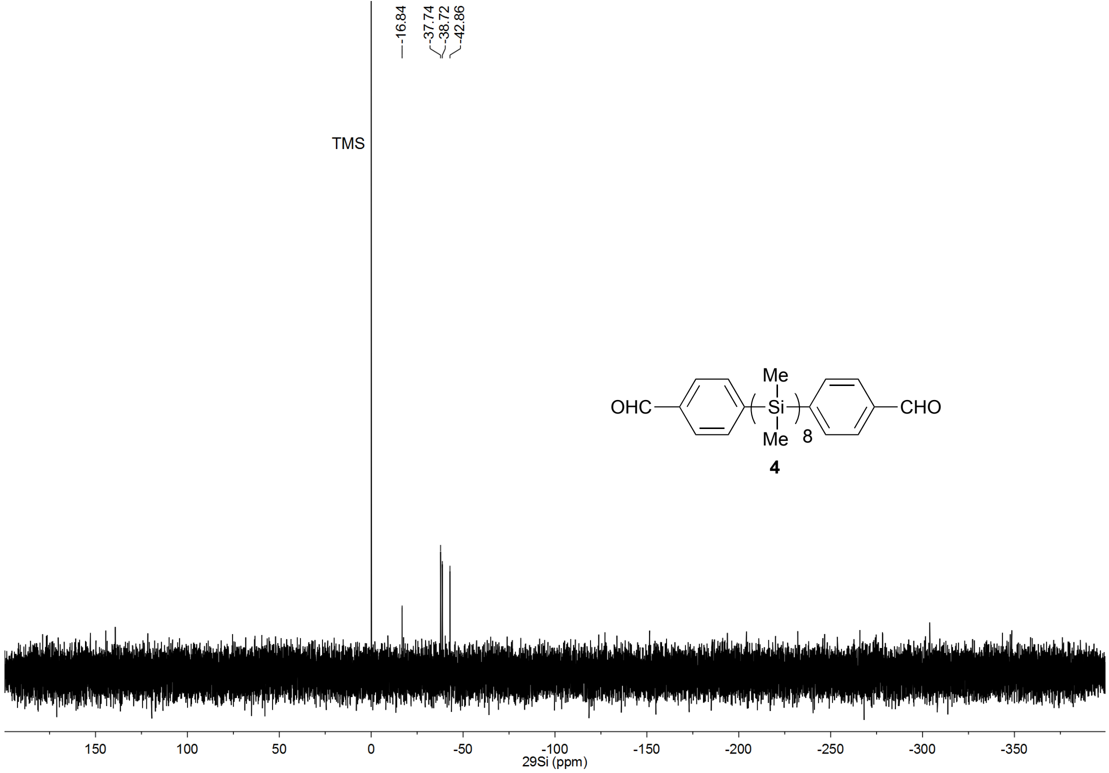

2.7 NMR Spectra of Compound **9**

2.7.1 ^{1}H NMR Spectrum (400 MHz, CDCl$_3$)

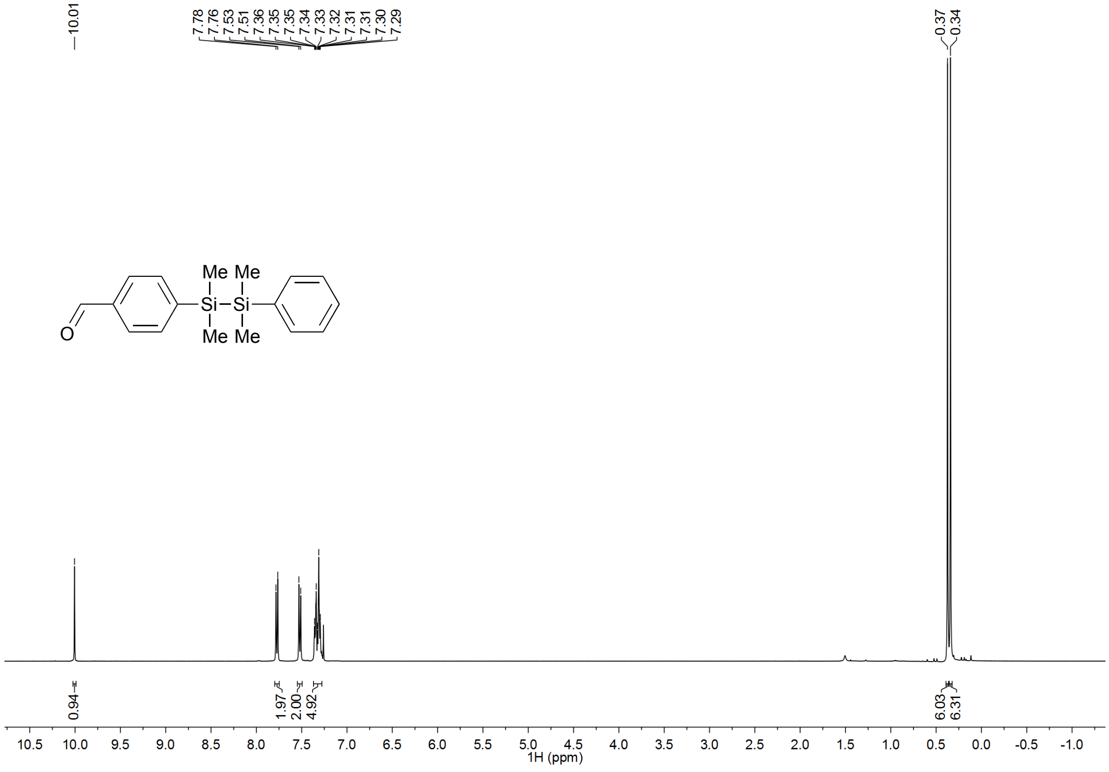

2.7.2 ^{13}C NMR Spectrum (101 MHz, $CDCl_3$)

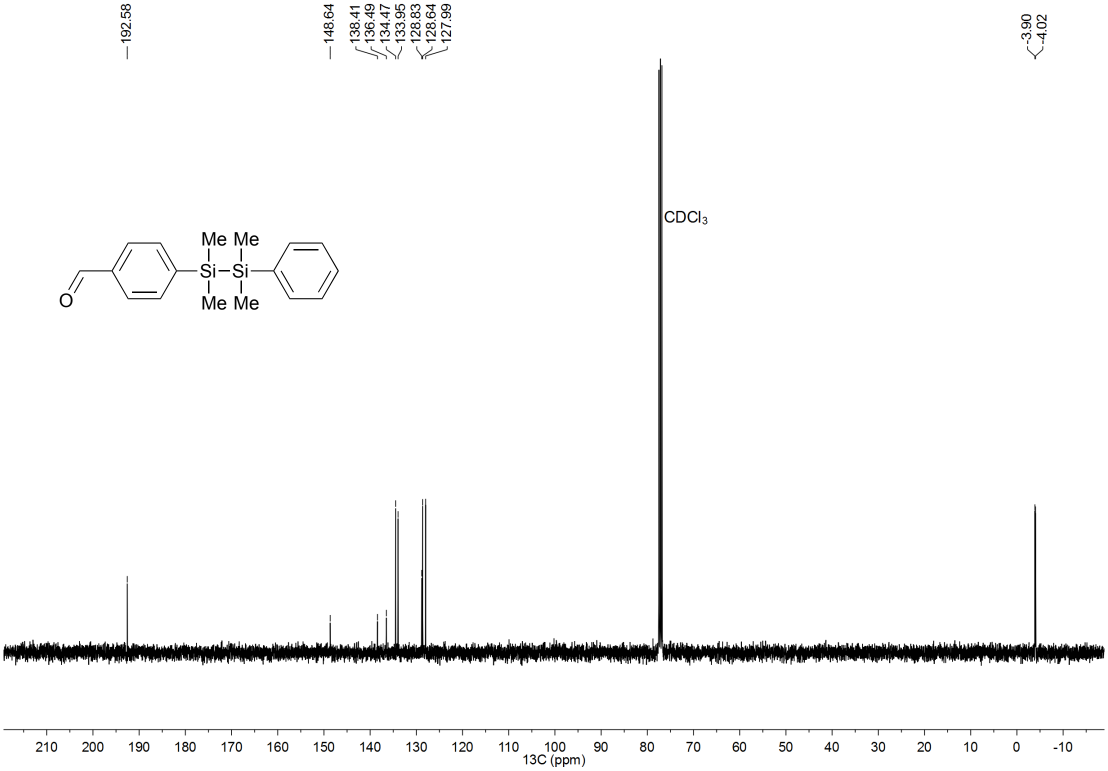

2.7.3 ^{29}Si NMR Spectrum (79 MHz, $CDCl_3$)

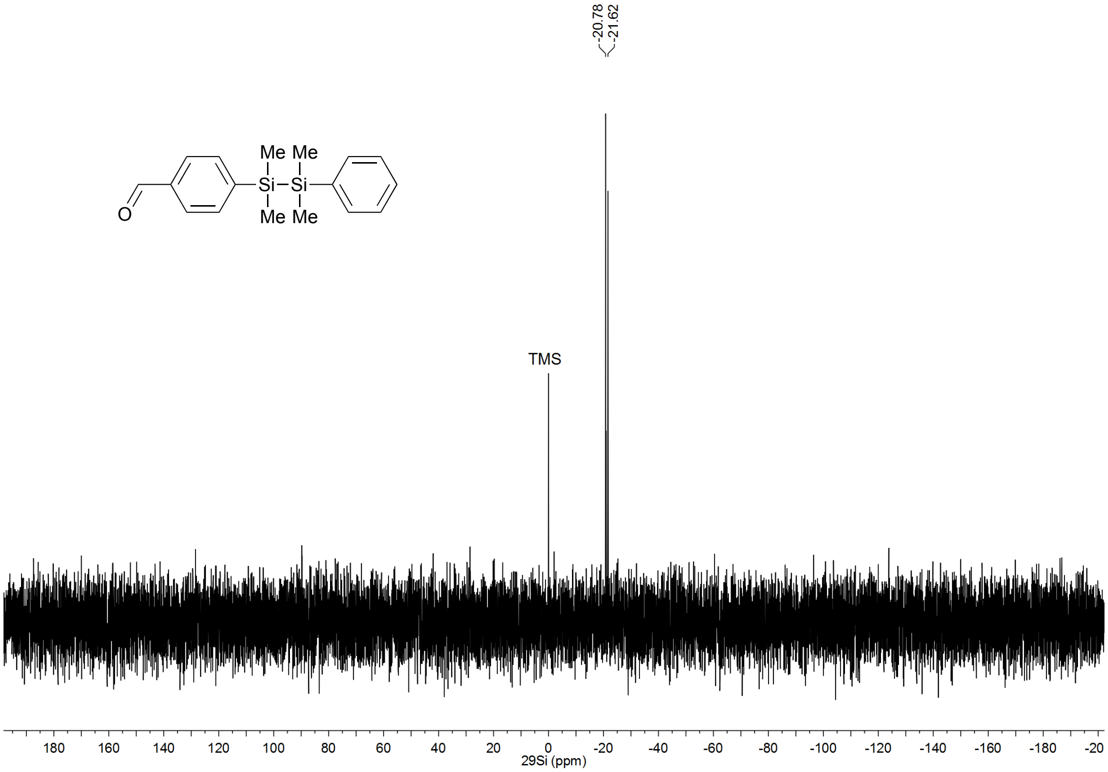

2.8 NMR Spectra of Compound **10**

2.8.1 ^{1}H NMR Spectrum (400 MHz, C_6D_6)

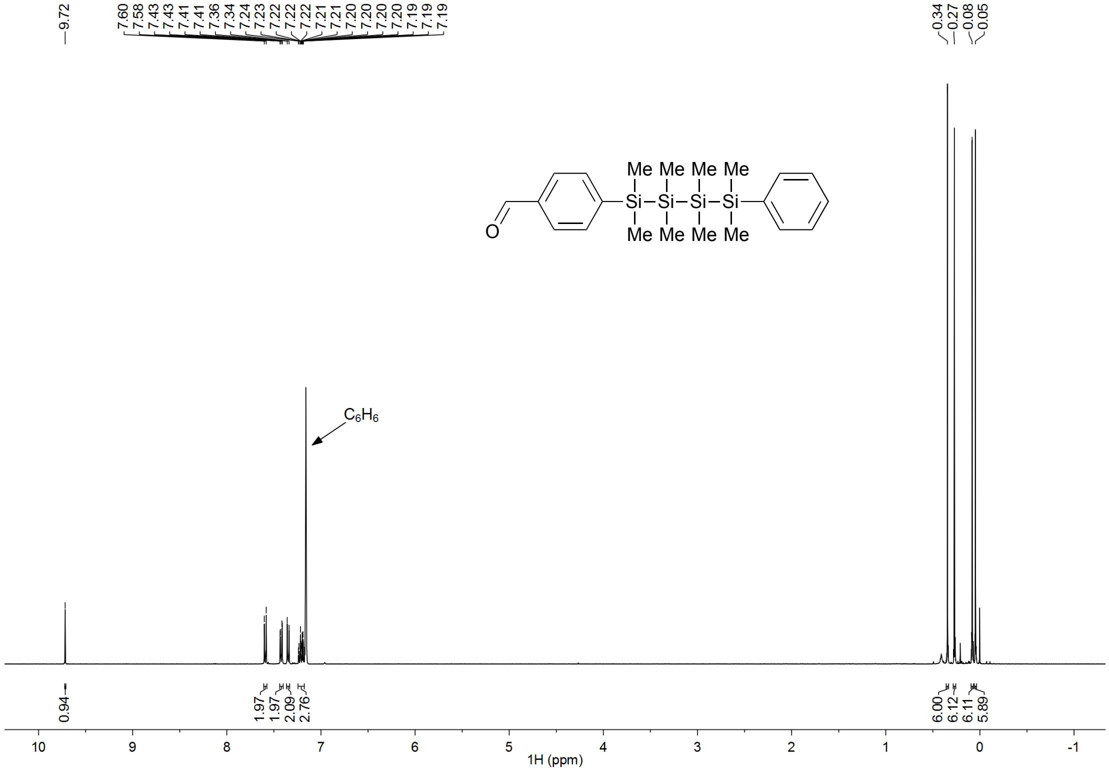

2.8.2 ^{13}C NMR Spectrum (75 MHz, $CDCl_3$)

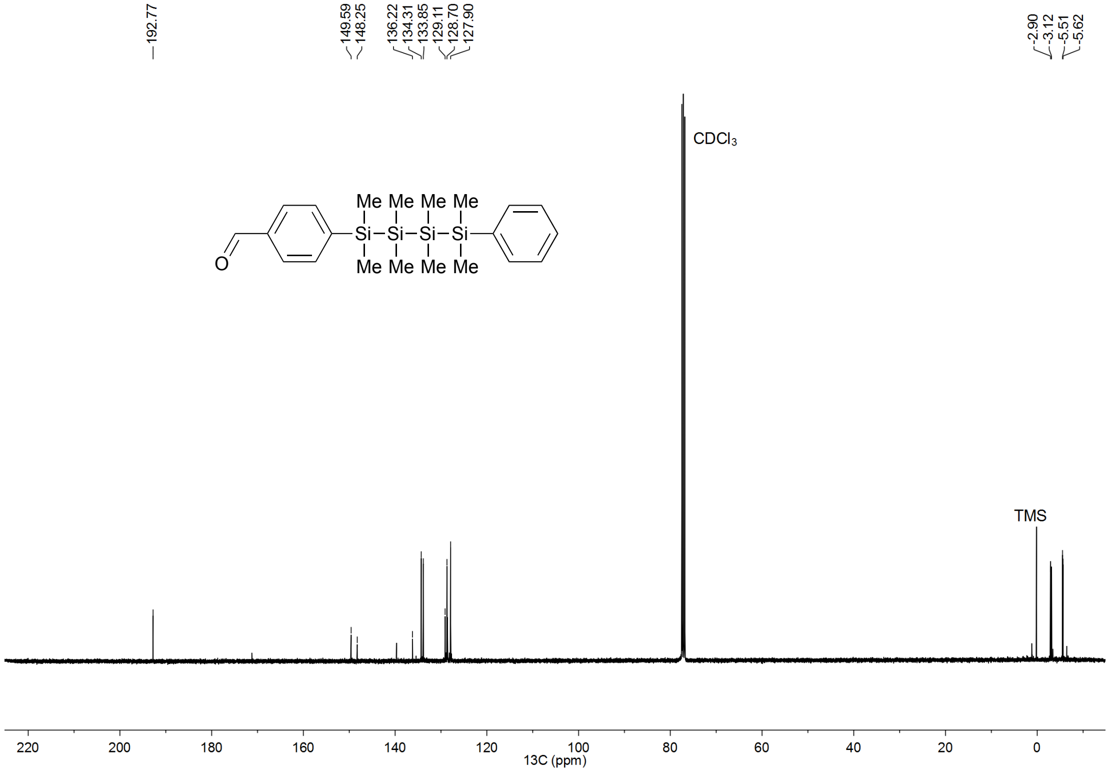

2.8.3 ^{29}Si NMR Spectrum (79 MHz, C_6D_6)

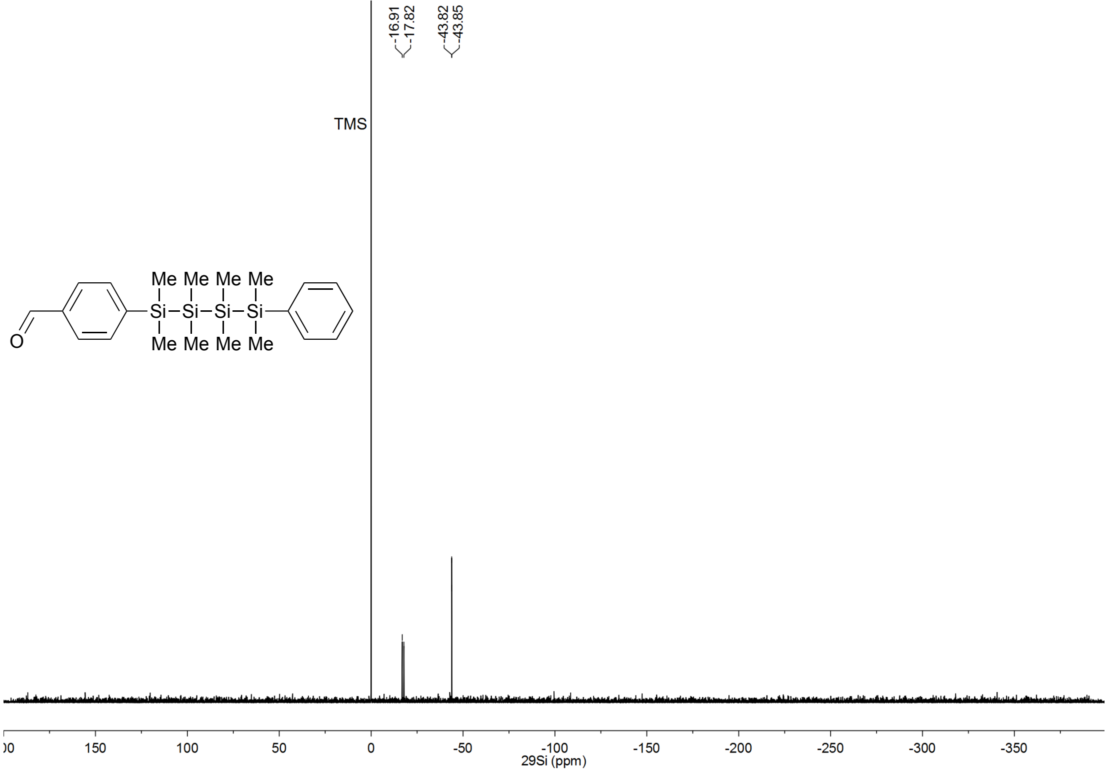

2.9 NMR Spectra of Compound **Si8s**

2.9.1 ^{1}H NMR Spectrum (400 MHz, $CDCl_3$)

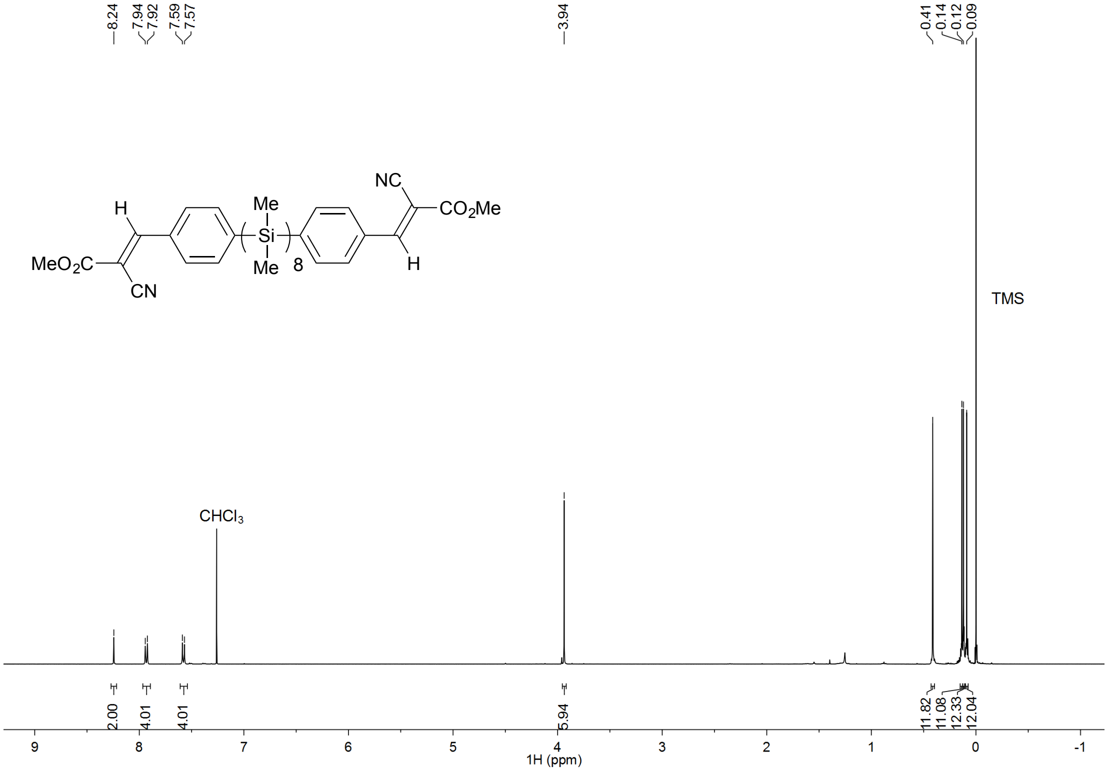

2.9.2 ^{13}C NMR Spectrum (101 MHz, CDCl$_3$)

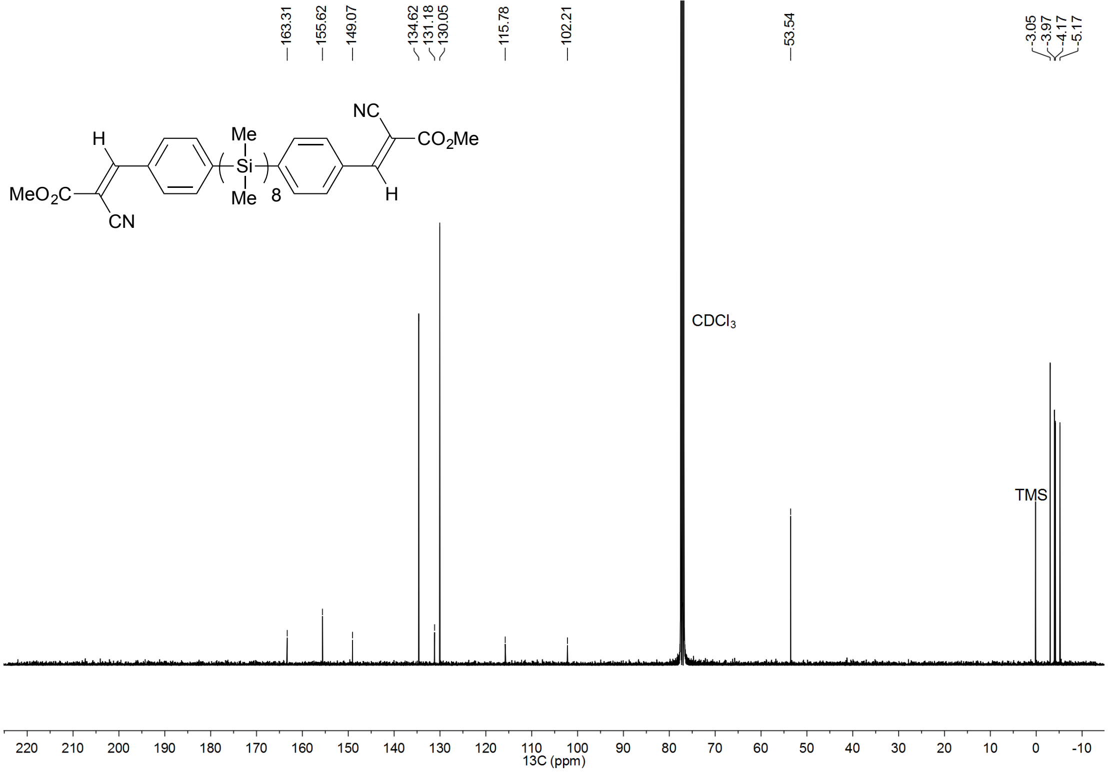

2.9.3 ^{29}Si NMR Spectrum (79 MHz, CDCl$_3$)

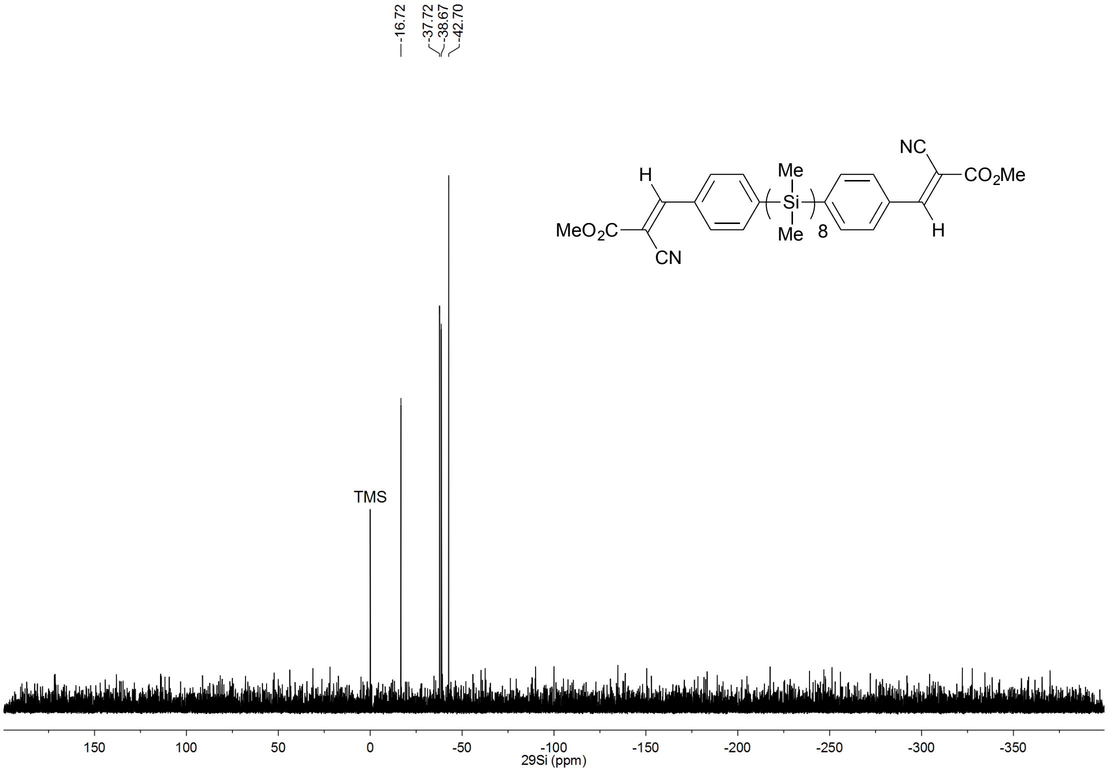

2.10 NMR Spectra of Compound **Si2a**

2.10.1 ^{1}H NMR Spectrum (400 MHz, CDCl$_3$)

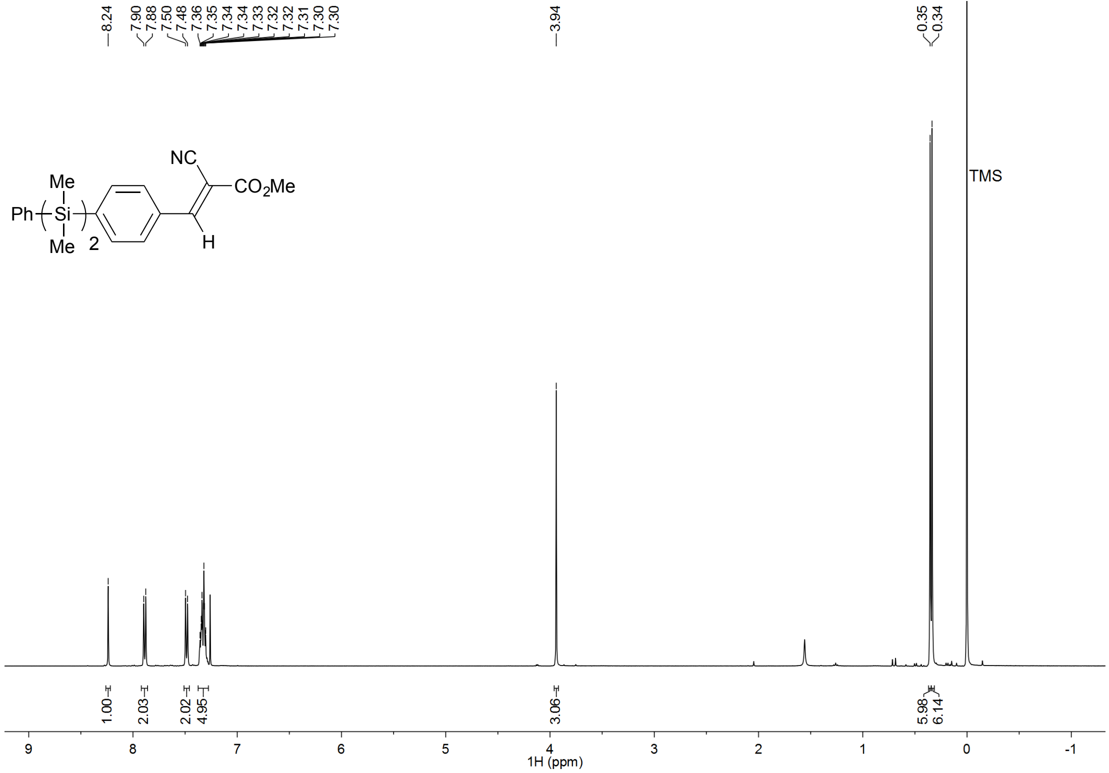

2.10.2 ^{13}C NMR Spectrum (101 MHz, CDCl$_3$)

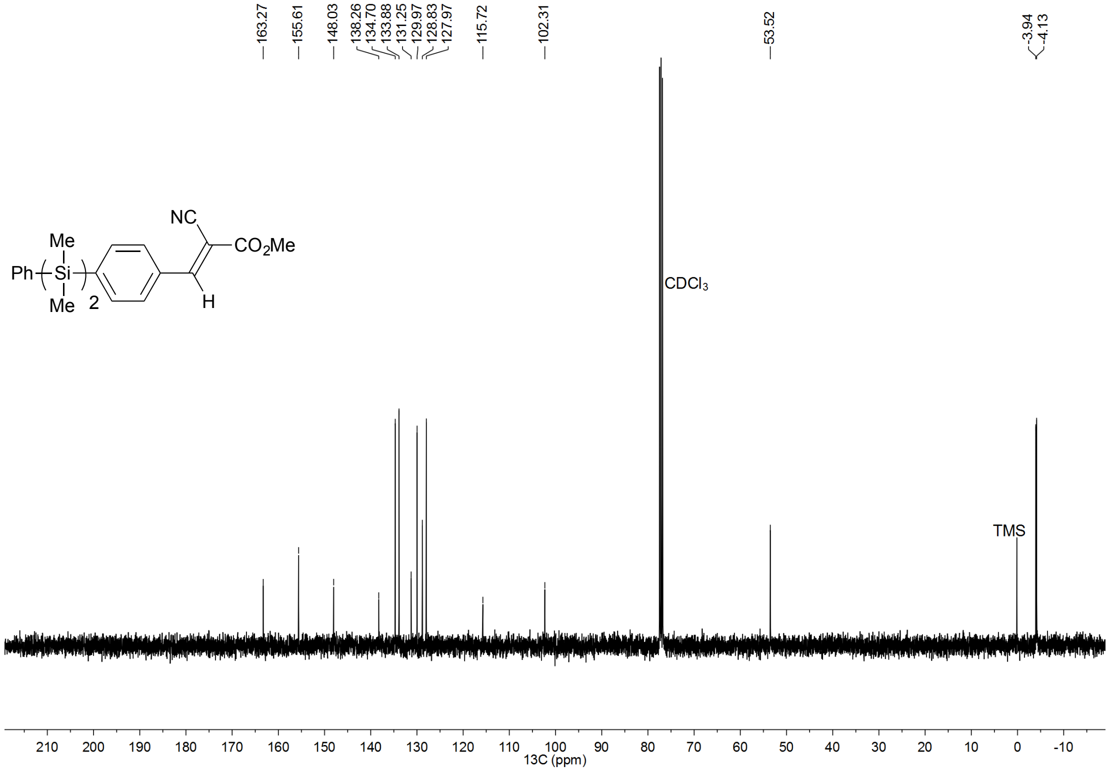

2.10.3 ^{29}Si NMR Spectrum (79 MHz, $CDCl_3$)

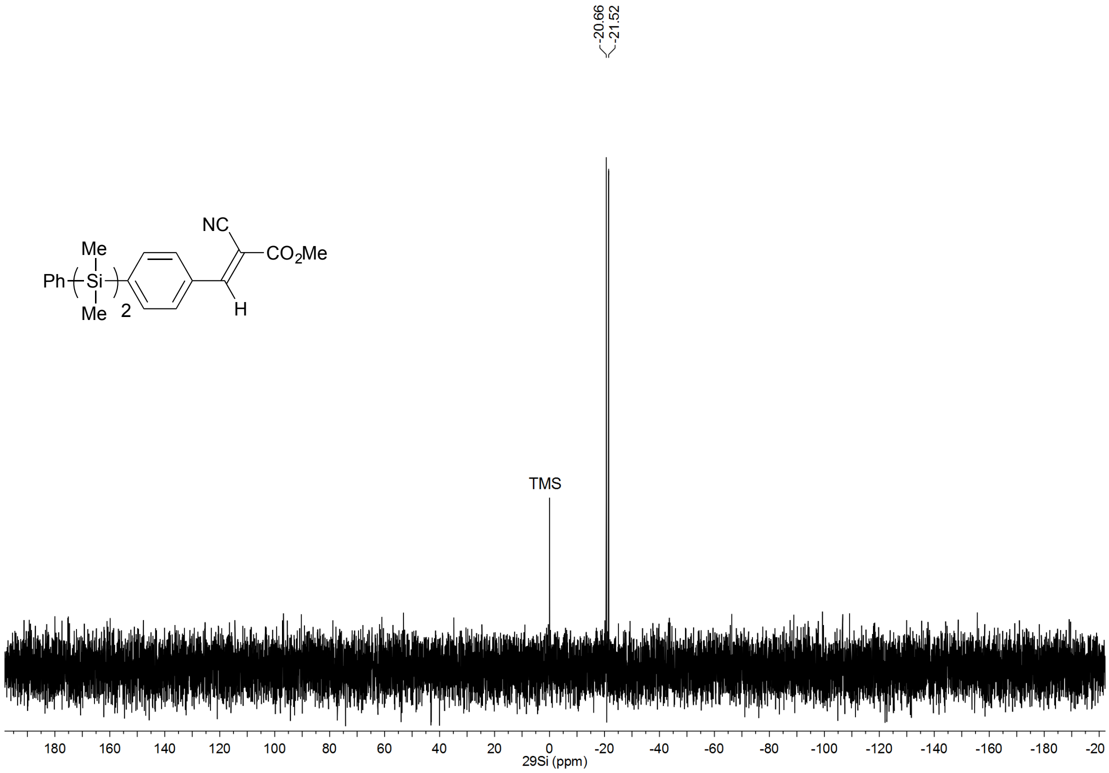

2.11 NMR Spectra of Compound **Si4a**

2.11.1 ^{1}H NMR Spectrum (400 MHz, $CDCl_3$)

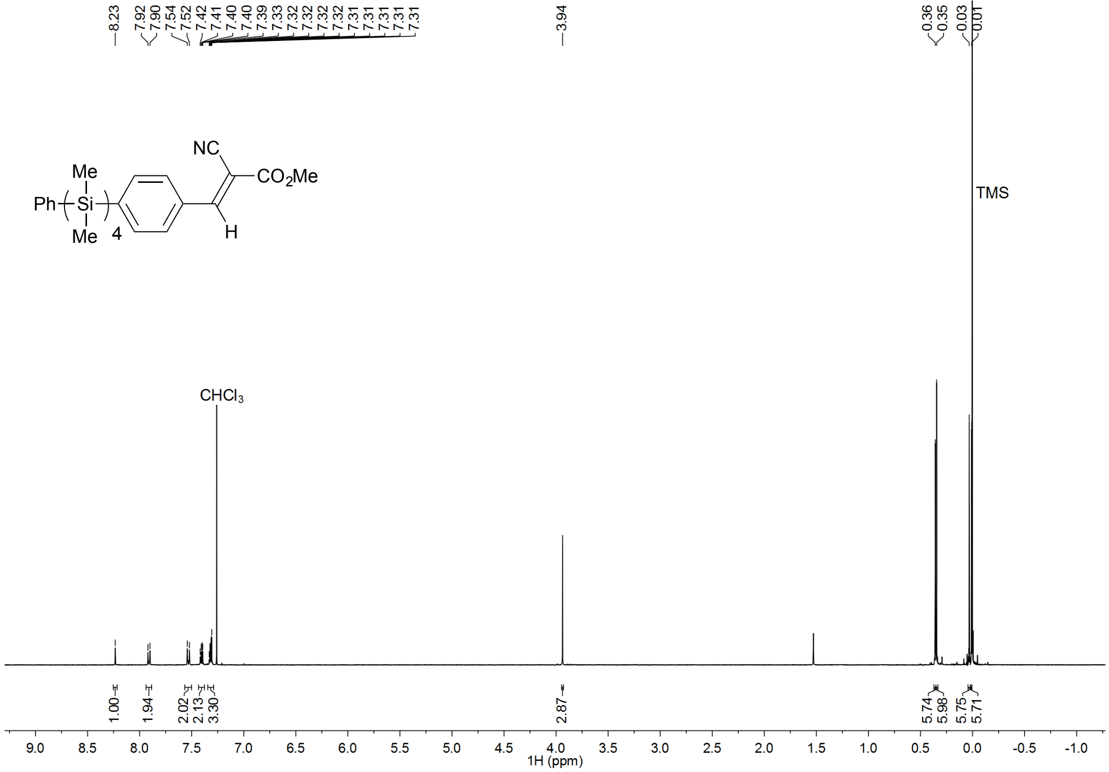

2.11.2 ^{13}C NMR Spectrum (101 MHz, CDCl$_3$)

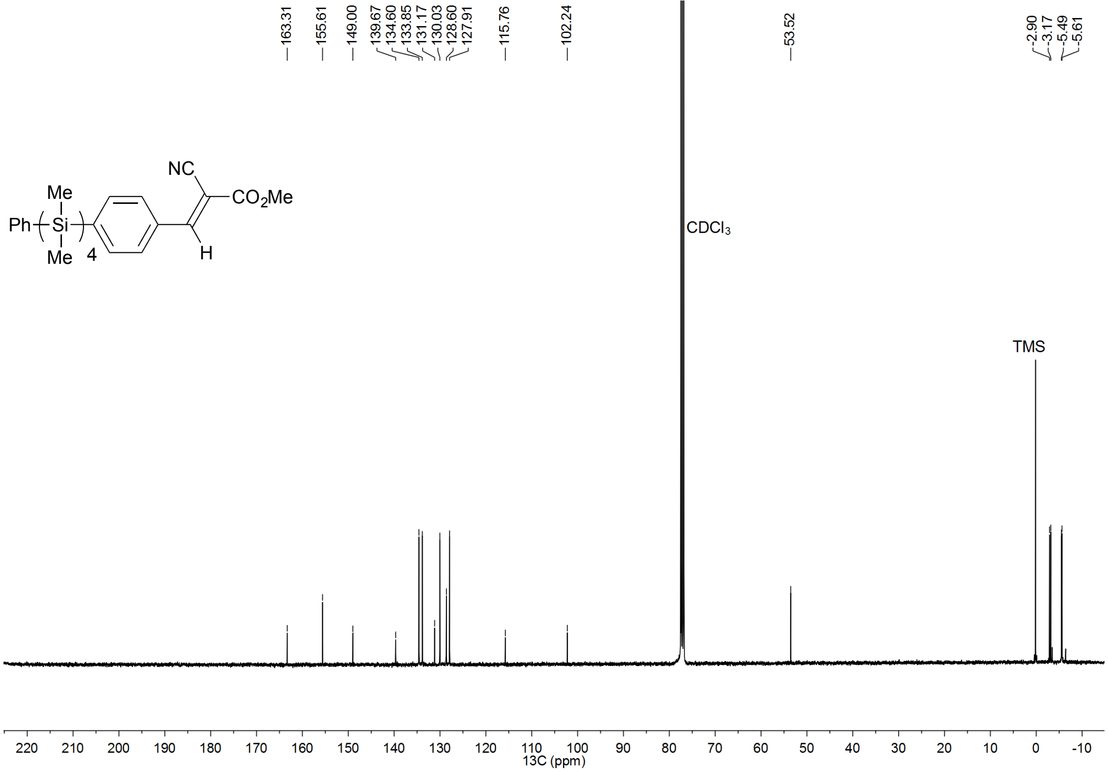

2.11.3 ^{29}Si NMR Spectrum (79 MHz, CDCl$_3$)

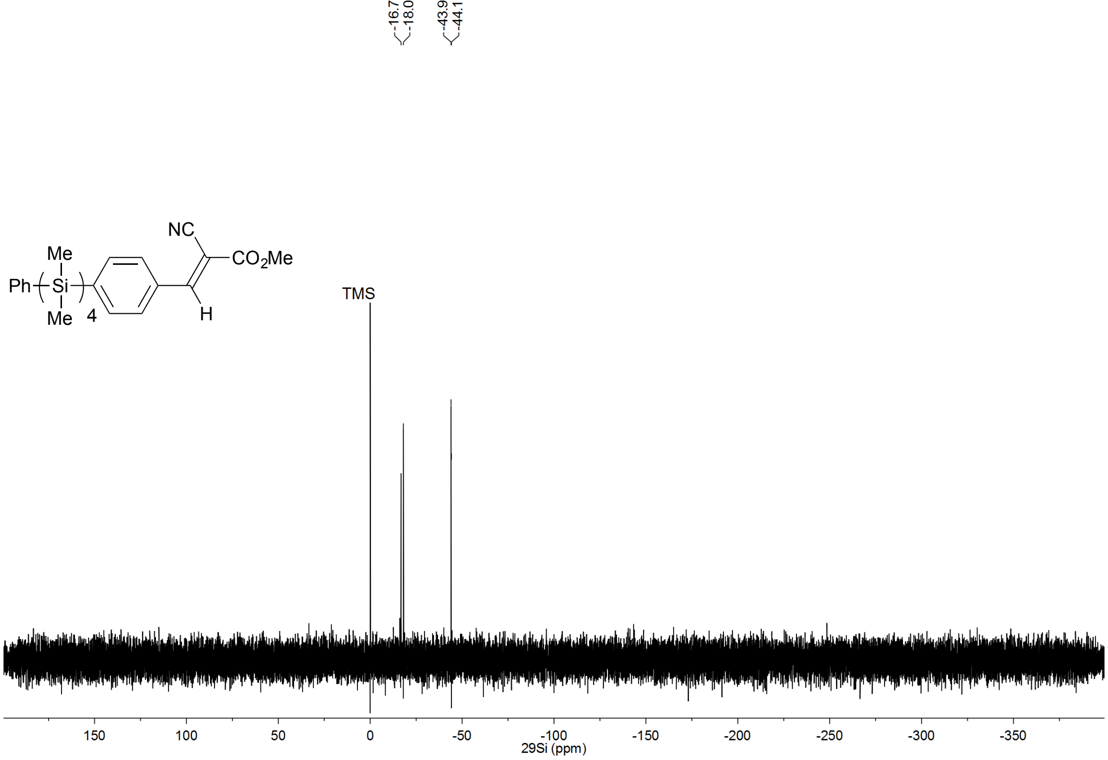

3. Supplemental Figures

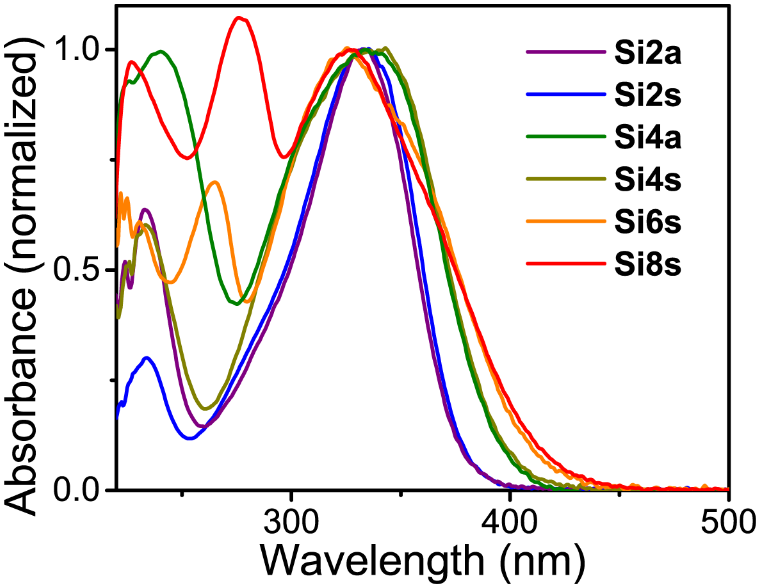

Figure S1. UV-Vis absorption spectra of **Si*n*s** (*n*=2-8) and **Si*n*a** (2,4) in CH_2Cl_2.

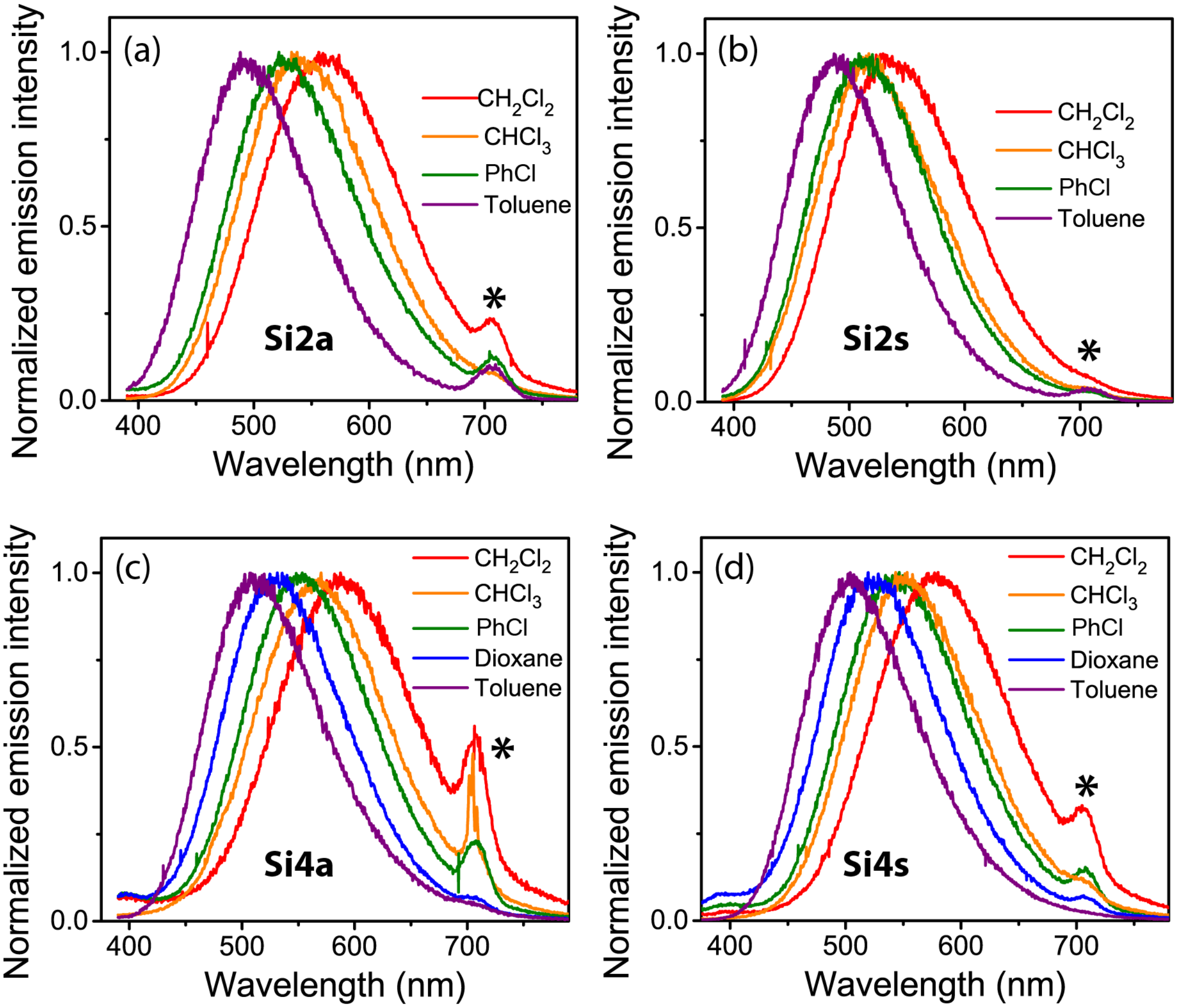

Figure S2. Dispersed fluorescence from (a) **Si2a**, (b) **Si2s**, (c) **Si4a** and (d) **Si4s** in various solvents. * denotes second-order diffraction of scatter from the excitation source (360 nm).

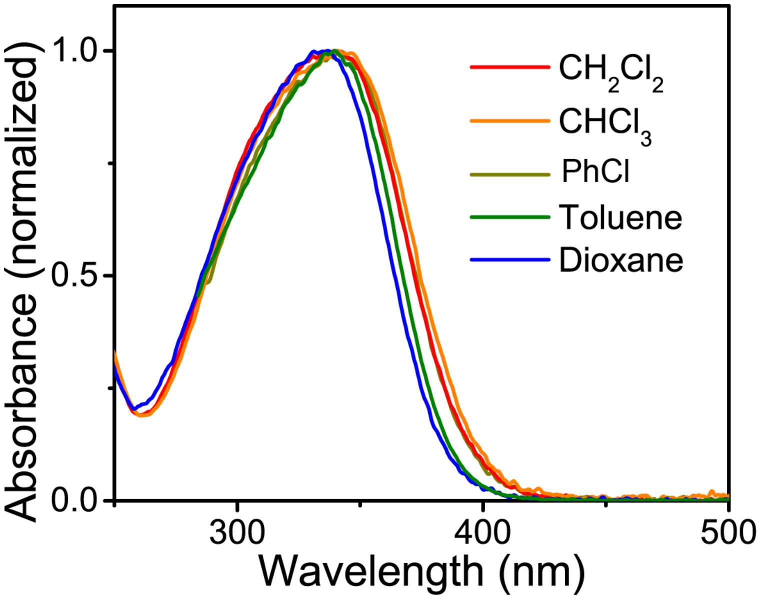

Figure S3. Comparison of steady-state absorption of **Si4s** in various solvents. Only weak solvatochromism (~10 nm) is observed for all compounds at the absorption onset (onset taken as 10% peak absorbance).

Table S1. Solvent properties for Lippert analysis of solvochromatic Stokes shift.

Solvent	Dielectric constant (ε)	Refractive index (n)	Δf
Toluene	2.38	1.4969	0.01324
Dioxane	2.25	1.4224	0.02451
Chlorobenzene (ArCl)	5.62	1.5248	0.14294
Chloroform ($CHCl_3$)	4.81	1.4458	0.14829
DCM (CH_2Cl_2)	8.93	1.4241	0.21714

Table S2. Lippert Analysis of solvochromatic Stokes shift from **Si*n*s** and **Si*n*a**.

Compound	$\Delta\bar{\nu}_0$ (cm^{-1})[a]	Slope	a (Å)[b]	$\Delta\mu$ (D)
Si2a	6420 ± 380	9510 ± 2550	8.3	23 ± 3
Si2s	6060 ± 260	6990 ± 1730	11.4	32 ± 4
Si4a	6650 ± 460	4970 ± 3040	8.7	18 ± 6
Si4s	6090 ± 360	6880 ± 2710	8.7	21 ± 4
Si6s	6220 ± 350	7310 ± 2650	10.5	29 ± 5

[a] Extrapolated Stokes shift for absence of solvent.
[b] Determined from calculated structures of organosilanes.

Table S3. Solubility of organosilanes in various solvents.

	Si2a	Si2s	Si4a	Si4s	Si6s
Toluene	Y	Y	-	Y	Y
Dioxane	N	N	Y	Y	Y
Chlorobenzene (ArCl)	Y	Y	Y	Y	N
Chloroform ($CHCl_3$)	Y	Y	Y	Y	Y
DCM (CH_2Cl_2)	Y	Y	Y	Y	Y

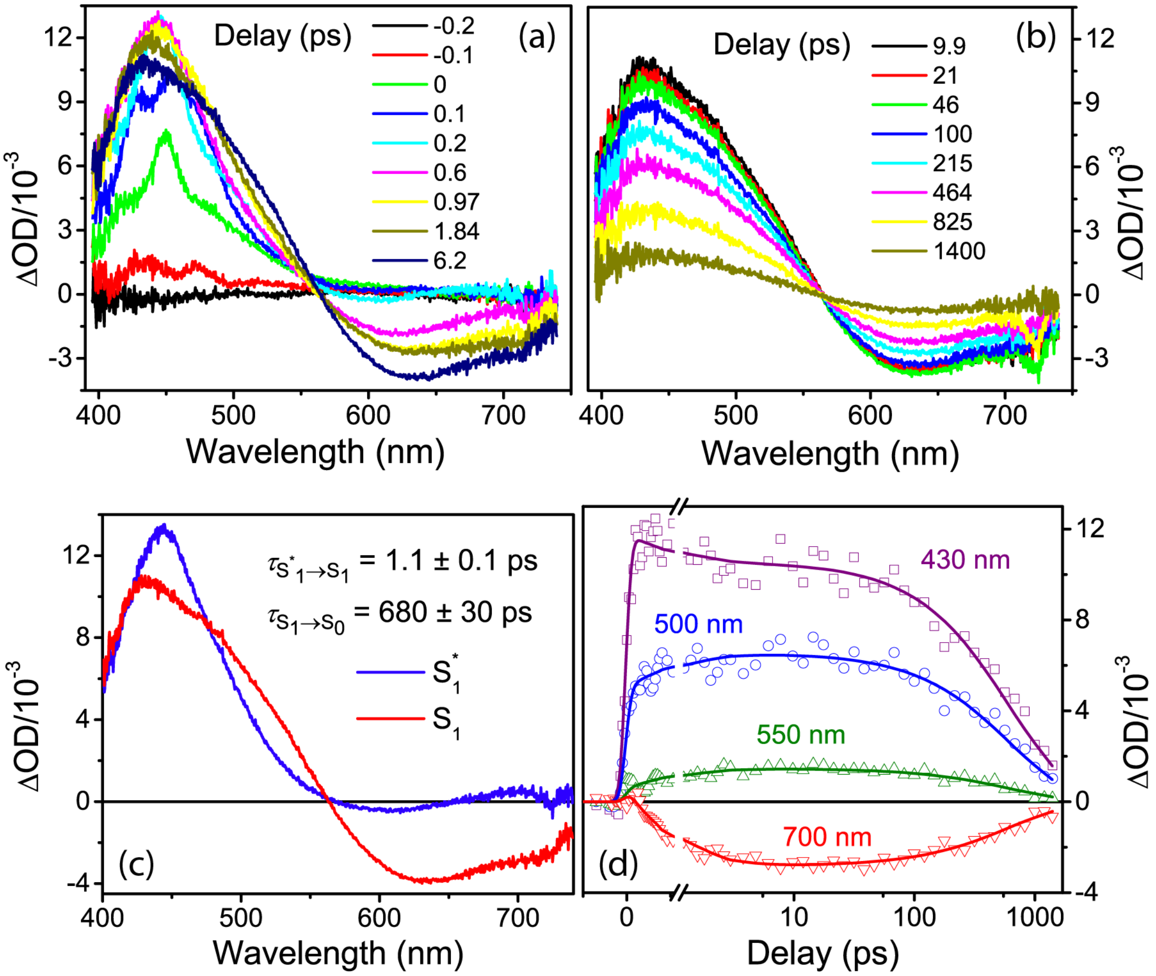

Figure S4. TA spectra of **Si2s** in CH_2Cl_2 following 360-nm excitation (a) before and (b) after 7 ps. (c) Species associated spectra and (d) fits to kinetic model (equation 2 of main text) at selected wavelengths obtained using global analysis.

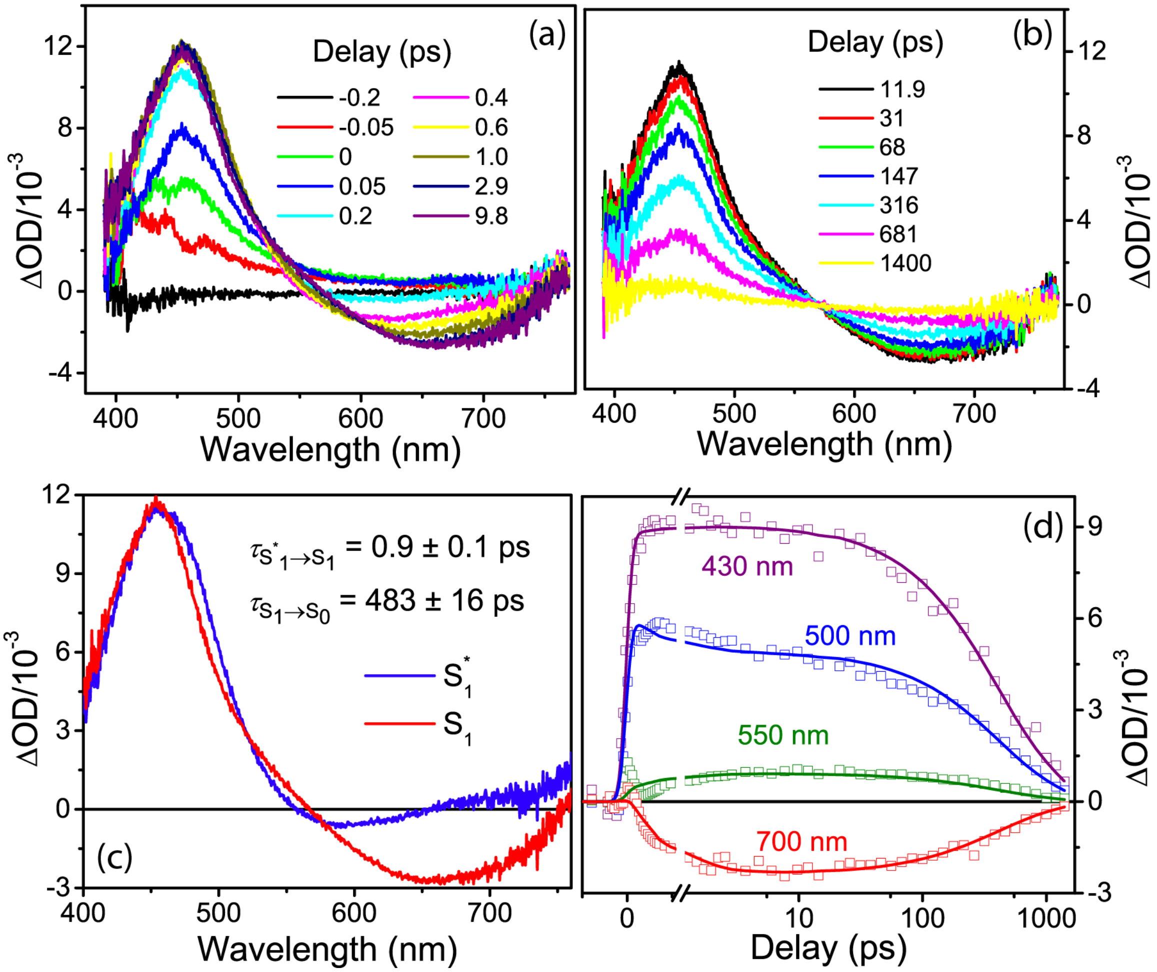

Figure S5. TA spectra of **Si2a** in CH_2Cl_2 following 360-nm excitation (a) before and (b) after 10 ps. (c) Species associated spectra and (d) fits to kinetic model (equation 2 of main text) at selected wavelengths obtained using global analysis.

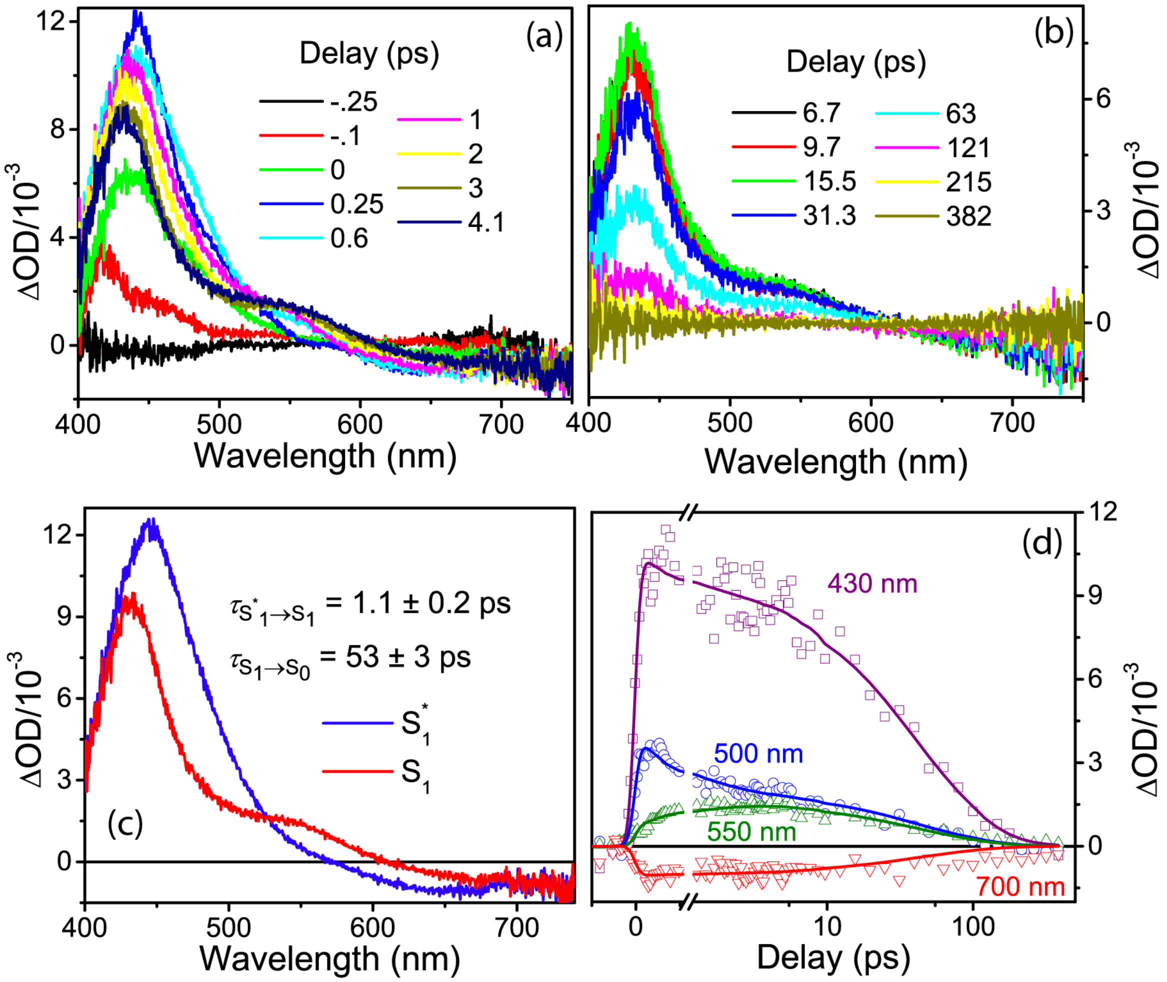

Figure S6. TA spectra of **Si6s** in CH_2Cl_2 following 360-nm excitation (a) before and (b) after 5 ps. (c) Species associated spectra and (d) fits to kinetic model (equation 2 of main text) at selected wavelengths obtained using global analysis.

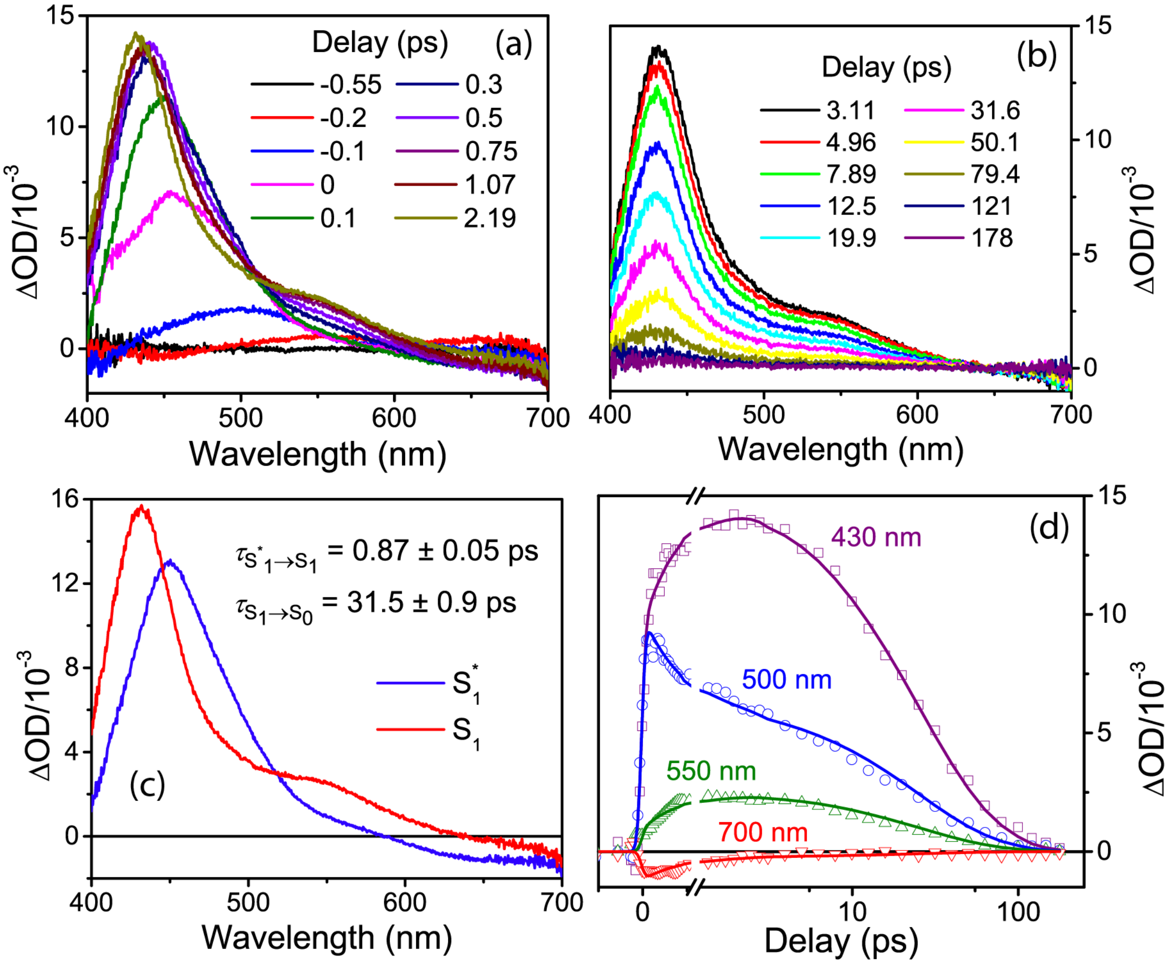

Figure S7. TA spectra of **Si8s** in CH_2Cl_2 following 360-nm excitation (a) before and (b) after 3 ps. (c) Species associated spectra and (d) fits to kinetic model (equation 2 of main text) at selected wavelengths obtained using global analysis.

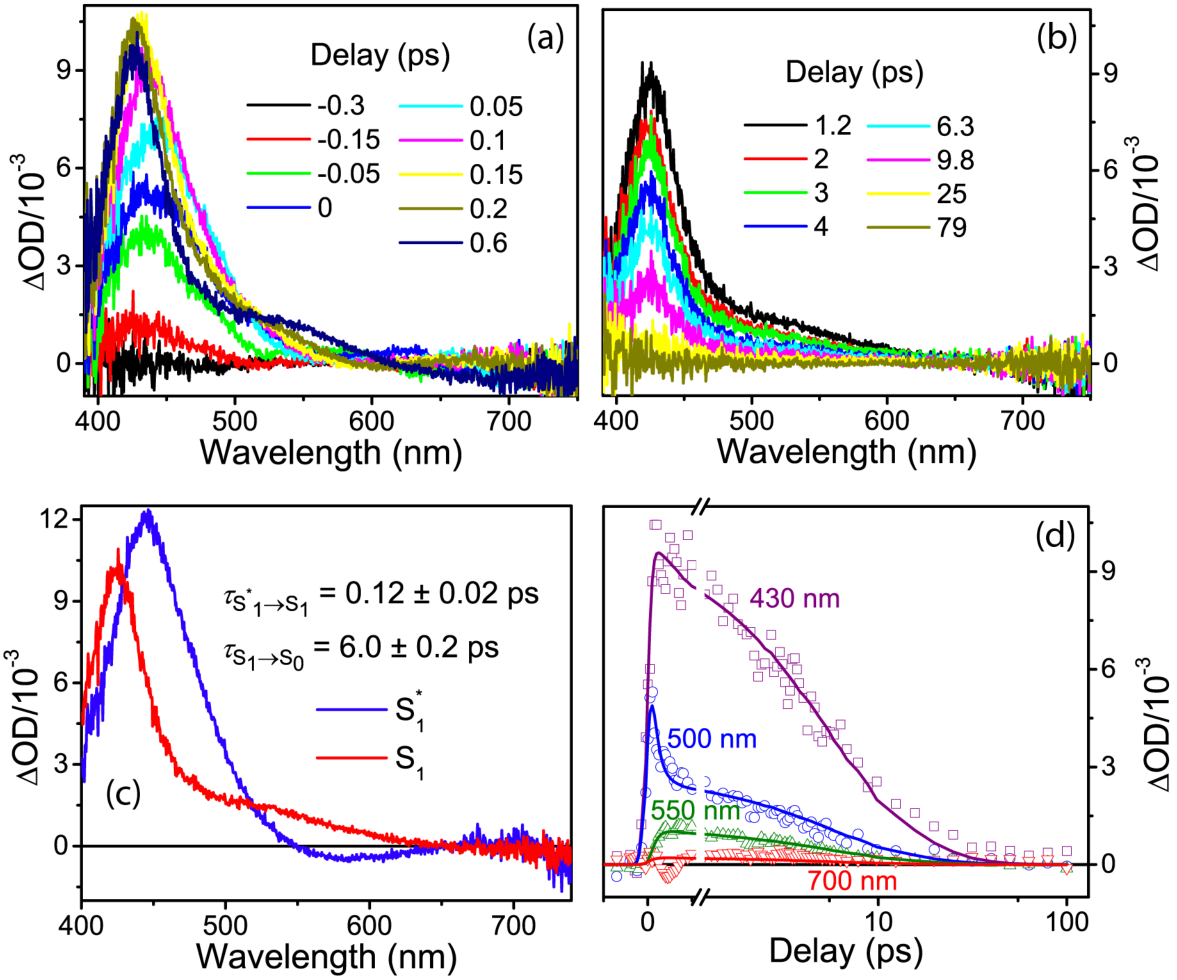

Figure S8. TA spectra of **Si6s** in acetonitrile following 360-nm excitation (a) before and (b) after 1 ps. (c) Species associated spectra and (d) fits to kinetic model (equation 2 of main text) at selected wavelengths obtained using global analysis.

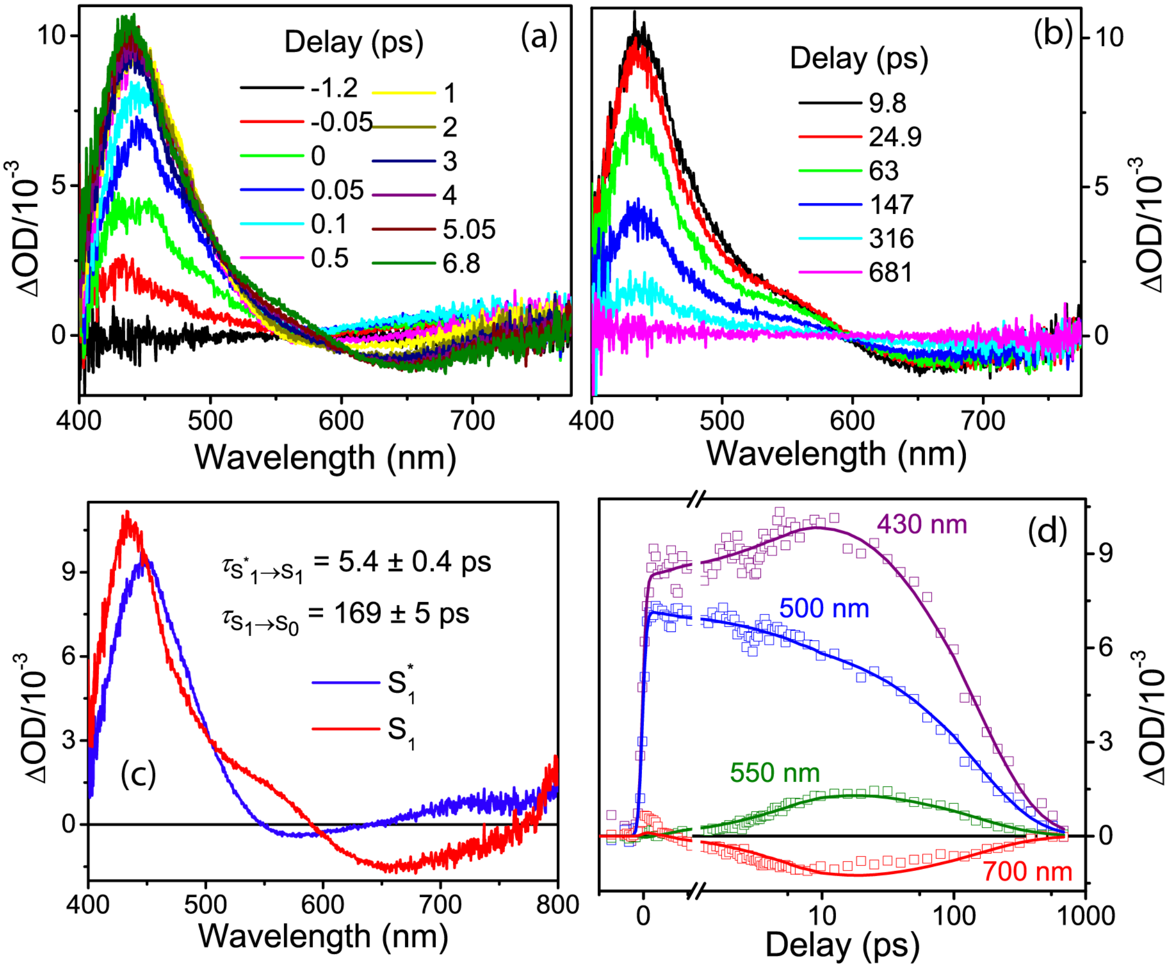

Figure S9. TA spectra of **Si6s** in chloroform following 360-nm excitation (a) before and (b) after 7 ps. (c) Species associated spectra and (d) fits to kinetic model (equation 2 of main text) at selected wavelengths obtained using global analysis.